



---

All Theses and Dissertations

---

2008-08-11

# Cellular and Matrix Changes in Articular Cartilage of the Disproportionate micromelia Mouse Model of Osteoarthritis

Crystal Noelle Smaldone  
*Brigham Young University - Provo*

Follow this and additional works at: <https://scholarsarchive.byu.edu/etd>

 Part of the [Cell and Developmental Biology Commons](#), and the [Physiology Commons](#)

---

## BYU ScholarsArchive Citation

Smaldone, Crystal Noelle, "Cellular and Matrix Changes in Articular Cartilage of the Disproportionate micromelia Mouse Model of Osteoarthritis" (2008). *All Theses and Dissertations*. 1636.  
<https://scholarsarchive.byu.edu/etd/1636>

This Thesis is brought to you for free and open access by BYU ScholarsArchive. It has been accepted for inclusion in All Theses and Dissertations by an authorized administrator of BYU ScholarsArchive. For more information, please contact [scholarsarchive@byu.edu](mailto:scholarsarchive@byu.edu), [ellen\\_amatangelo@byu.edu](mailto:ellen_amatangelo@byu.edu).

CELLULAR AND MATRIX CHANGES IN ARTICULAR CARTILAGE  
OF THE DISPROPORTIONATE MICROMELIA MOUSE  
MODEL OF OSTEOARTHRITIS

by

Crystal N. Smaldone

A thesis submitted to the faculty of

Brigham Young University

in partial fulfillment of the requirements for the degree of

Master of Science

Department of Physiology and Developmental Biology

Brigham Young University

December 2008

BRIGHAM YOUNG UNIVERSITY

GRADUATE COMMITTEE APPROVAL

of a thesis submitted by

Crystal N. Smaldone

This thesis has been read by each member of the following graduate committee and by majority vote has been found to be satisfactory.

\_\_\_\_\_  
Date

\_\_\_\_\_  
Robert E. Seegmiller, Chair

\_\_\_\_\_  
Date

\_\_\_\_\_  
John S. Gardner

\_\_\_\_\_  
Date

\_\_\_\_\_  
Jeffery R. Barrow

BRIGHAM YOUNG UNIVERSITY

As chair of the candidate's graduate committee, I have read the thesis of Crystal N. Smaldone in its final form and have found that (1) its format, citations, and bibliographical style are consistent and acceptable and fulfill university and department style requirements; (2) its illustrative materials including figures, tables, and charts are in place; and (3) the final manuscript is satisfactory to the graduate committee and is ready for submission to the university library.

---

Date

---

Robert E. Seegmiller  
Chair, Graduate Committee

Accepted for the Department

---

James P. Porter  
Department Chair

Accepted for the College

---

Rodney J. Brown  
Dean, College of Life Sciences

## ABSTRACT

### CELLULAR AND MATRIX CHANGES IN ARTICULAR CARTILAGE OF THE DISPROPORTIONATE MICROMELIA MOUSE MODEL OF OSTEOARTHRITIS

Crystal Noelle Smaldone

Department of Physiology and Developmental Biology

Master of Science

Osteoarthritis (OA) is a degenerative joint disease that affects more than 60% of Americans 65 and older. Because human subjects and samples are not readily available for research, animal models are an invaluable resource for the study of OA. Disproportionate micromelia (Dmm) is one such model that develops OA early in life due to a deletion in the c-propeptide of the *Col2a1* gene. Light microscope analysis of the articular cartilage in Dmm has been completed, but is insufficient to show the cellular effects of the deletion mutation in Dmm in adequate detail. The present study explores the changes that occur in the rough endoplasmic reticulum (ER) of chondrocytes in the articular cartilage of Dmm heterozygous mutants (D/+). Immunohistochemical analysis in Dmm has shown that type II collagen is absent extracellularly in articular cartilage of Dmm homozygous mutants and reduced in the

heterozygotes. Because procollagens are processed through the endoplasmic reticulum (ER), it has been hypothesized that due to improper folding this mutation prevents newly synthesized collagen from leaving the ER, as a result large dilations are seen in the ER of Dmm mice. Furthermore, matrix area fractions should be reduced in the D/+ group if indeed type II collagen is not secreted. Data collected indicated that at 4 months and older, large dilations in the ER disappear. At age 0 months, there is significant dilation in the ER of the D/+ ( $p=.0013$ ), and at .75 months significant dilation is also observed ( $p=.0063$ ). In pooled age groups, the D/+ has a 1.77% greater ER fraction than the +/+ ( $p=.0022$ ). The matrix area fraction was also significantly lower in the D/+ compared to the +/+ ( $p=.0037$ ). Apoptosis was prominent in older ages, but did not appear to be different between +/+ and D/+ mice. Because decreased matrix and dilation of ER have been documented in OA, Dmm is a good model of OA that can be further used to study the molecular changes and deficiencies that occur in the pathogenesis of OA.

## ACKNOWLEDGEMENTS

This page is an insufficient means of thanking all of the wonderful people that have changed my life in my time as a graduate student. First, I would like to thank the members of my committee for their support and guidance. Dr. Seegmiller, thank you for letting me be your graduate student. Dr. Gardner, I, like many that have worked with you, am indebted to you for all of your help and too owe you my first-born (Can we cut a deal on that?). Even though you had no obligations to me, you were willing to lift me up on the long, tough days that come with being a graduate student. You are an invaluable friend, and the world needs more people like you. Dr. Barrow, thank you for being a kind, compassionate mentor. You are a teacher extraordinaire. I loved being your TA and hope that one day I can give lectures and care about my students as you do.

I am indebted to so many others in the microscopy lab. Mike, you are the ultimate sectioning machine. Thanks for your patience with all of my “stuff” spread in various locations of the lab and for teaching me all of the TEM techniques I needed. I want to thank all those who willingly gave up their time to help me with eleventh-hour analysis: Haylee Stewart, Nettina Smith, Rob Holmes, Melissa Baker, and Gideon Burrows. Thanks to the cheerleading squad of moral supporters in the lab: Marta Adair, Darren Hodges, Dr. Richard Heckmann, and Dr. Paul Urie. Lastly, thanks Mom and Dad; I love you and could not have done it without your encouragement and support.

# TABLE OF CONTENTS

<b>INTRODUCTION .....</b>	<b>1</b>
<b>ARTICULAR CARTILAGE .....</b>	<b>1</b>
<b>OSTEOARTHRITIS.....</b>	<b>3</b>
<b>DISPROPORTIONATE MICROMELIA (DMM) .....</b>	<b>4</b>
<b>APOPTOSIS.....</b>	<b>6</b>
<b>DMM AS A MODEL FOR OSTEOARTHRITIS .....</b>	<b>7</b>
<b>METHODS AND MATERIALS.....</b>	<b>9</b>
<b>FACILITIES AND ANIMAL MANAGEMENT.....</b>	<b>9</b>
<b>GENOTYPING .....</b>	<b>9</b>
<b>TISSUE ACQUISITION AND PROCESSING.....</b>	<b>10</b>
<b>LIGHT AND ELECTRON MICROSCOPY .....</b>	<b>11</b>
<b>MICROSCOPIC ANALYSIS .....</b>	<b>12</b>
<i>ER AREA FRACTION.....</i>	<i>12</i>
<i>CELL AND MATRIX AREA FRACTIONS .....</i>	<i>13</i>
<i>APOPTOSIS .....</i>	<i>14</i>
<b>STATISTICAL ANALYSIS.....</b>	<b>14</b>
<b>RESULTS.....</b>	<b>16</b>
<b>CELL AND MATRIX AREA FRACTIONS .....</b>	<b>16</b>
<i>GENOTYPE COMPARISON FOR ALL AGES .....</i>	<i>16</i>
<i>GENOTYPE COMPARISON WITHIN AGES.....</i>	<i>19</i>
<i>AGE COMPARISON WITHIN GENOTYPES.....</i>	<i>23</i>
<b>ER AREA FRACTION .....</b>	<b>25</b>
<i>GENOTYPE COMPARISON WITHIN AGES.....</i>	<i>27</i>
<b>APOPTOSIS.....</b>	<b>39</b>
<b>DISCUSSION &amp; FUTURE STUDIES.....</b>	<b>40</b>
<b>AREA FRACTIONS (ER, MATRIX, CELL) .....</b>	<b>40</b>
<b>APOPTOSIS.....</b>	<b>43</b>
<b>BIBLIOGRAPHY .....</b>	<b>45</b>



## LIST OF FIGURES

FIGURE 1: LAYERS OF ARTICULAR CARTILAGE .....	2
FIGURE 2: SCHEMATIC DIAGRAM OF A GEL . .....	10
FIGURE 3: SCHEMATIC DIAGRAM OF A LEFT KNEE JOINT .....	11
FIGURE 4: LIGHT MICROGRAPH OF THE KNEE JOINT.....	12
FIGURE 5: DIAGRAM ILLUSTRATING ER AREA FRACTION ANALYSIS .....	13
FIGURE 6: DIAGRAM ILLUSTRATING HOW CELL/MATRIX AREA FRACTION ANALYSIS. ....	14
FIGURE 7: AREA FRACTIONS BY GENOTYPE.....	16
FIGURE 8: LIGHT MICROGRAPHS OF ARTICULAR CARTILAGE AT ALL AGES.....	17
FIGURE 9: TRANSMISSION ELECTRON MICROGRAPHS FOR ALL AGES (TOP LEFT).....	18
FIGURE 10: BAR GRAPHS FOR CELL AREA FRACTIONS AT EACH AGE.....	21
FIGURE 11: BAR GRAPHS OF MATRIX AREA FRACTIONS AT EACH AGE.....	22
FIGURE 12: CELL AREA FRACTION COMPARISON OVER TIME.....	24
FIGURE 13: MATRIX AREA FRACTION COMPARISON OVER TIME .....	25
FIGURE 14: BAR GRAPHS OF ER FRACTIONS IN ALL DEPTHS WITH AGES POOLED .....	26
FIGURE 15: MATRIX AND ER TEM AT 0 MONTHS. ....	28
FIGURE 16: ER AREA FRACTION AT 0 MONTHS (MIDDLE DEPTH) .....	29
FIGURE 17: BAR GRAPHS OF ER FRACTIONS AT ALL AGES IN MIDDLE CELLS.....	29
FIGURE 18: TEM OF MIDDLE CHONDROCYTES AT 0.75 MONTHS .....	31
FIGURE 19: TEM OF MIDDLE CHONDROCYTES AT 1.5 MONTHS.....	32
FIGURE 20: TEM OF MIDDLE CHONDROCYTES AT 4 MONTHS .....	33
FIGURE 21: TEM OF MIDDLE CHONDROCYTES AT 7 MONTHS .....	34
FIGURE 22: ER AREA FRACTION CHANGES WITH AGE.....	36
FIGURE 23: TEM OF CHANGES IN THE SUPERFICIAL MATRIX.....	37
FIGURE 24: LESIONS IN THE SUPERFICIAL MATRIX.....	38
FIGURE 25: APOPTOTIC CELL.....	39

## LIST OF TABLES

TABLE 1: AREA FRACTION COMPARISON BY GENOTYPE (AGES COMBINED) .....	16
TABLE 2: AREA FRACTION COMPARISONS BY GENOTYPE WITHIN AGES .....	20
TABLE 3: AREA FRACTION COMPARISONS IN +/+ MICE ACROSS AGES .....	23
TABLE 4: AREA FRACTION COMPARISONS IN D/+ MICE ACROSS AGES .....	24
TABLE 5: ER AREA FRACTION COMPARISON BY GENOTYPE (AGES COMBINED) .....	26
TABLE 6: ER AREA FRACTION COMPARISONS BY GENOTYPE AT 0 MONTHS .....	27
TABLE 7: ER AREA FRACTION COMPARISONS BY GENOTYPE WITHIN AGES .....	35
TABLE 8: ER AREA FRACTION COMPARISONS WITHIN GENOTYPES AND ACROSS AGES .....	36
TABLE 9: APOPTOSIS CELL COUNTS IN 6 REPLICATES .....	39

## INTRODUCTION

### **Articular Cartilage**

Articular cartilage is a layer of smooth hyaline cartilage found at the ends of the long bones. Articular cartilage's main role is to absorb tensile and compressive stresses placed on the joints.<sup>1-4</sup> This connective tissue is composed of chondrocytes (cartilage cells) supported by a unique scaffold of collagens, proteoglycans, and non-collagenous proteins that form the extracellular matrix (ECM). Chondrocytes are the only cell type found in the articular cartilage and are responsible for synthesizing the ECM proteins.<sup>2,5</sup> Because ECM proteins are continually degraded and renewed throughout the life of an individual, the health and proper function of the chondrocytes is essential for maintaining articular cartilage.

With regard to dealing with mechanical stresses such as tensile forces, collagens are a key element of articular cartilage. The 28 collagens that have been described fall into two major classes: fibril forming and non-fibril forming. Type II collagen, a fibril forming collagen, is the primary collagen and most abundant protein in articular cartilage.<sup>2,3,6-8</sup> Mature type II collagen is a homotrimer of polypeptides wrapped together in an alpha-helix. It begins as a pre-procollagen with amino- and carboxy-propeptides and a signal sequence. Once the signal sequence is cleaved, the procollagen chains associate in trimers in the endoplasmic reticulum (ER) of chondrocytes. These procollagens are then processed through the golgi apparatus and secreted into the matrix where the amino and carboxy-terminus propeptides are cleaved by N- and C-proteinases respectively.<sup>5-12</sup> The final product is a latticework of mature collagen fibrils that gives articular cartilage its shape and ability to withstand shearing forces. Collagen is further

supported by proteoglycans, a protein core with polysaccharide chains, and other non-collagenous proteins.<sup>2,13-15</sup>

Four distinct layers of articular cartilage have been described: superficial, transitional, middle/deep, and calcified, but clear delineations are not visible

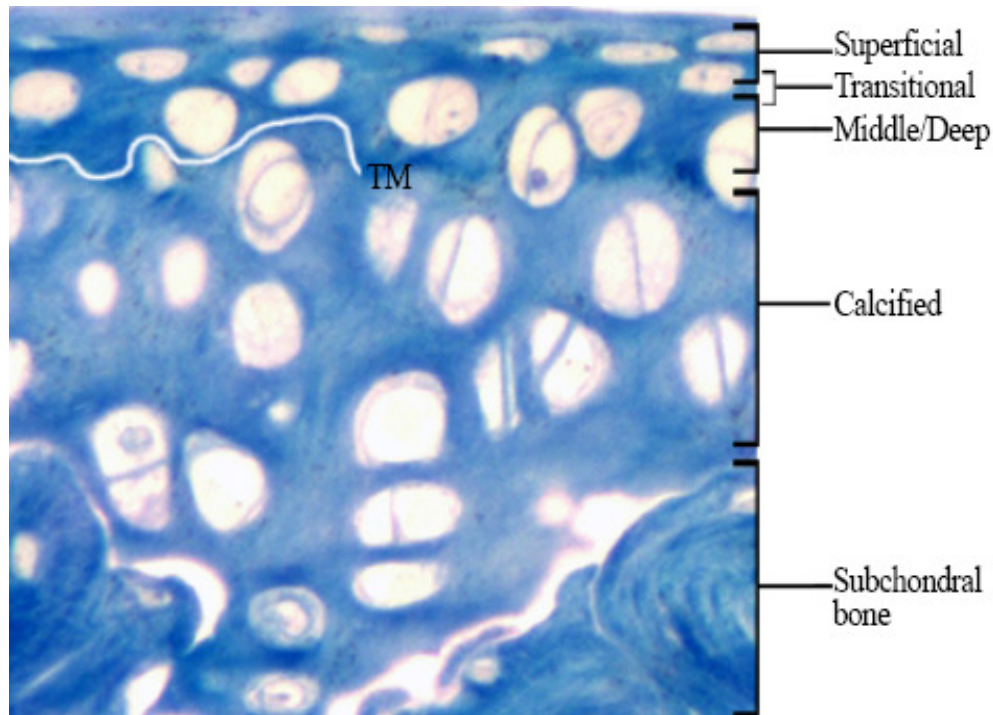


**Figure 1: Layers of articular cartilage**

The tidemark (TM) (partially enhanced in white) separates uncalcified from calcified cartilage. No other clear delineations are seen between layers.

between each of these layers (Figure 1). Although the elements of these layers are essentially the same, each has unique a function, morphology, and composition of matrix proteins.<sup>2</sup> Superficial chondrocytes are flat, spindle-shaped cells that run parallel to the articular surface along with the ECM.<sup>1</sup> Chondrocytes in this layer have a decreased amount of cytoplasmic organelles. The superficial matrix has an abundance of collagen and water and a lower proteoglycan content compared to other layers. These properties allow the superficial zone to give articular cartilage its shape and stiffness. Damage or

alterations to the superficial zone, manifest as fibrillations, are believed to be a major starting point in the onset of osteoarthritis.<sup>16-19</sup> The layer below the superficial layer is the transitional layer. Transitional cells are spheroidal and have abundant cytoplasmic organelles. Matrix fibrils in this layer run oblique to the cell surface, and the matrix has lower collagen and water content than the superficial layer and increased proteoglycan. The middle/deep zone has a columnar arrangement of cells, low water content, and high proteoglycan concentration. Cells of the middle zone lie right along the tide mark (Figure 1), a border between calcified and uncalcified cartilage. Calcified cartilage is the layer below the tidemark and superficial to the subchondral bone. Cells in this layer are usually smaller than in the other layers and have fewer cytoplasmic organelles.<sup>2</sup> In the described layers, cartilage continually undergoes metabolic, biochemical and structural changes based on stresses placed on the joints. Healthy maintenance of articular cartilage is dependent on a balance of anabolic and catabolic processes. When this balance is disturbed, one degenerative joint disease that can develop is osteoarthritis.<sup>2,3,18,20,21</sup>

### **Osteoarthritis**

Osteoarthritis (OA) is the most common form of arthritis, affecting more than 60% of Americans 65 and older.<sup>22</sup> This disease is manifest when homeostasis is not maintained in the articular cartilage. OA is manifest by the breakdown of articular cartilage, commonly displayed in the knee joints. In the beginning stages of OA, the articular cartilage degenerates, leading to pain and discomfort. Over time a more significant portion of the articular cartilage may be lost, which results in spurs on the bone surface due to hardening of the subchondral bone.<sup>19,22</sup> Eventually, the integrity of

the cartilage may become compromised to the point that it degenerates completely, leaving bare femoral chondyles rubbing against a bare tibial surface.

Initial changes in the articular cartilage that lead to OA are postulated to occur in the superficial layer. Fibrillation of the superficial layer increases the permeability of the articular cartilage, allowing changes in the osmolarity and water content of the cartilage. As indicated above, as water content increases in cartilage the concentration of proteoglycans and other matrix proteins decreases. These biochemical changes lead to decreased tensile strength.<sup>13-15,17</sup>

OA does not typically reach severe stages in a short period of time. Chondrocytes are constantly maintaining the articular cartilage by sensing biochemical changes in the matrix through connections with the ECM. As a result of increased water or decreased matrix protein concentration, the cells shift to an anabolic state in an attempt to maintain proper concentrations of matrix proteins and the osmolarity of the tissue.<sup>3,13,23</sup> Severe OA only develops when catabolic processes in the cartilage are disproportionately increased compared to anabolic processes. In many cases, temporary improvements are seen in the articular cartilage following onset of OA, and the disease may progress over many years.<sup>20,22</sup> This illustrates a strong age component in the development of OA, but aging is not the sole cause of OA. Primary OA occurs when a specific disease cause is unknown (i.e. aging), whereas secondary OA occurs when a specific cause is known: joint trauma or injury, genetic pre-disposition, infection, and metabolic factors.<sup>15,17</sup>

### **Disproportionate micromelia (Dmm)**

One specific source of secondary OA is mutation of the *Col2a1* gene because it codes for type II collagen, which, as previously stated, is the most prominent collagen in

articular cartilage. A large variety of mutations has been documented in *Col2a1* with similar and sometimes identical disease phenotypes including several collagenopathies: Stickler syndrome,<sup>24</sup> Kniest dysplasia, spondyloepithelial dysplasia congenital,<sup>6</sup> achondrogenesis,<sup>25</sup> osteoarthritis (OA).<sup>12</sup> Unfortunately, the use of human subjects for OA research is limited; therefore, the quest for better treatments of the disease is hindered. Instead, researchers rely on animal models that carry mutations in *Col2a1* to better understand the molecular mechanisms that lead to the onset and progression of OA.

Murine models, therefore, are a precious resource that facilitates continuing research to determine the molecular pathways that play a role in the pathogenesis of OA; one such model is Disproportionate micromelia (Dmm). The mutant gene carries a three-nucleotide deletion in the c-propeptide coding region of *Col2a1* gene that causes an Asn to replace what is Lys and Thr in the wild-type.<sup>12</sup> As a result of the mutation, the Col2a1 chains are not properly assembled, which leads to defective collagen assembly, leading to the manifestation of mutant phenotypes. As reviewed above, the c-propeptide is cleaved upon secretion into the extracellular matrix. In Dmm homozygotes, it is uncertain whether pro-collagens even form and are secreted.

Two distinct phenotypes are observed in Dmm: homozygous mutant (D/D) and heterozygous mutant (D/+). D/D mice are characterized by a cleft palate and severe chondrodysplasia; in fact, the mutation is lethal and the animals die of pulmonary hypoplasia at birth.<sup>26</sup> Heterozygotes have mildly decreased length of limbs, tail, and body in addition to the onset of OA by four months postpartum.<sup>27-30</sup> Since histological studies demonstrate that D/+ mice develop OA, it has become an invaluable model for studying the molecular mechanisms that lead to OA in humans.

Previous studies on D/+ mice provide several clues as to how OA progresses in articular cartilage. Histological studies on D/+ mice at 3 and 6 months show that the articular cartilage is thinner, has an increased cell density and decreased matrix fraction compared with the wild-type.<sup>30</sup> The lack of type II collagen in the ECM is the presumed factor that leads to the manifestation of OA, but the mechanisms that cause a lack of collagen and increased chondrocyte density in articular cartilage are not known. Seegmiller et al. recently showed decreased matrix fraction, hypertrophy of chondrocytes, and dilation of the endoplasmic reticulum (ER) in fetal rib cartilage of Dmm, suggesting that the decreased matrix fraction may be due to the Col2a1 not being properly processed and released from the chondrocytes.<sup>31</sup> In other studies on other Col2a1 mutants, OA models, and human OA, a decreased matrix fraction due to OA was also shown with ER dilation,<sup>15,32</sup> increased water content in the matrix,<sup>14,15,20</sup> fibrillation and lesions in the superficial zone,<sup>17</sup> increased cell fractions,<sup>14</sup> matrix disorganization,<sup>30</sup> increased intracellular lipids,<sup>15</sup> increased microtubules,<sup>15</sup> and cell clustering.<sup>14,20</sup>

### **Apoptosis**

Apoptosis is another mechanism that is suspected to play a critical role in the progression of OA.<sup>33-36</sup> Apoptosis is programmed cell death in which cells are signaled to die. Markers for apoptosis include cell shrinkage, membrane blebbing, chromatin condensation (pycnosis), and DNA fragmentation while the mitochondria appear relatively normal.<sup>37,38</sup> Necrosis and apoptosis are commonly interchanged erroneously, but necrosis is unprogrammed cell death. Necrotic cells are characterized by swelling of the cytoplasmic organelles, a trait which is not observed in apoptotic cells.<sup>38</sup> In the



present study, the present study explored apoptosis in Dmm because recent research suggests that osteoarthritic cartilage may progress through an apoptotic pathway.<sup>33,34,36,37</sup>

### **Dmm as a model for osteoarthritis**

The proposed study was designed to look for cellular differences at the ultrastructural level in D/+ compared to age-matched controls. Because, abnormalities were observed in the ER of D/+ mice in fetal rib cartilage,<sup>31</sup> changes in the ER were specifically observed and quantified in the present study. In addition, cell and matrix area fractions were quantified across several age groups, and a preliminary survey for apoptosis was conducted.

It was expected that the cellular ultrastructure of Dmm cartilage would be significantly different from that of the wild-type (+/+). Apoptosis was anticipated to be observed more frequently in the Dmm mutant, and at older ages. Also, it was expected that the ratio of ECM to cells would be lower in D/+, indicating that part of the pathogenesis of OA in Dmm is due to the lack of collagen matrix. One possible cause of insufficient ECM is that the Col2a1 alpha chains are not being properly processed to permit them to leave the endoplasmic reticulum. If the chains are prevented from being secreted, it was predicted that the ER in D/+ would be dilated compared to the +/+ as observed in pilot studies and other representations of OA.<sup>9,31,32</sup>

Therefore, to further validate Dmm as a model of OA, and to further understand the ultrastructural changes in the pathogenesis of OA, the following objectives were proposed in D/+ mice:

## Objectives

1. To quantitatively characterize the ER at the ultrastructural level in articular cartilage of D/+ mice
2. To determine the cell and matrix area fractions in D/+ mice at several ages
3. To determine if degeneration of articular cartilage in D/+ mice may include an apoptotic pathway.

## METHODS AND MATERIALS

### **Facilities and Animal Management**

The colony of CH3 mice carrying the *Col2a1* mutation was maintained at Brigham Young University's animal care facility. Mice were kept in steel cages housing up to four mice and fed a standard mouse diet (Harlan Teklad 8604) ad libitum.

Between zero days and one month postpartum, identification numbers were assigned to each mouse, depending on the age of the animal at tissue acquisition.

### **Genotyping**

Tail snips were taken from each animal between zero days and 5 weeks postpartum, and genomic DNA was isolated (ethanol precipitation method) for differentiating between mutants (D/+, D/D) and controls (+/+). DNA was amplified in 50 ul PCR reactions using primers that flank the Dmm mutation: forward 5'–GAGAGGGCTTGGGCAAATGG; reverse 5'–GGTTGGAAAGTGTTTGGGTCC (Invitrogen). After amplification, DNA was exposed to BcgI restriction enzyme (New England Biosystems) for 5 hours at 37°C. BcgI cuts upstream and downstream of its recognition site in Dmm mutants, excising a small 34 bp fragment.<sup>39</sup> No recognition site is present in the wild-type gene so only one band representing the amplified sequence is seen for wild-type animals. D/+ animals have the wild-type band because they have one good copy of the *Col2a1* gene, and a lower band representing the 34 bp excision. D/D animals have only one band representing the excision (Figure 2). Restricted DNA was run on a 2% agarose gel and visualized with a UV transilluminator.

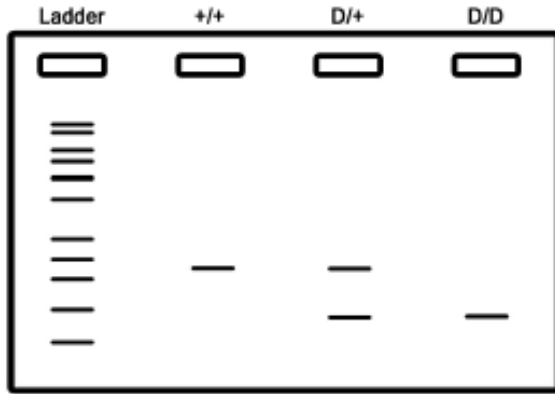


**Figure 2: Schematic diagram of a gel** showing how genotypes were determined.

### Tissue Acquisition and Processing

Tissues were collected from wild-type and D/+ animals at various ages (0, 0.75, 1.5, 4, 7, and 9 months). Because homozygous mutants only survive a few minutes past birth,<sup>26</sup> D/D samples were only included in the 0 months

age-group. Animals were first asphyxiated in a carbon-dioxide chamber, and the left knee joints were surgically removed and immediately fixed in 3% phosphate buffered glutaraldehyde (pH 7.4) overnight in preparation for transmission electron microscopy (TEM). Following fixation, knee joints from animals 0.75 months and older were decalcified in 14% EDTA for 5-7 days. Ascorbic acid was the initial decalcifying agent, and was found to be quite harsh on the tissue and caused morphological destruction of many cellular organelles including the ER. After fixation, each knee was sagittally cut, and the tibia and femur were trimmed closer to the joint (Figure 3). Lateral condyles were discarded, and medial condyles were washed with buffer, and stained with osmium tetroxide, and stained with uranyl acetate en block, dehydrated in an ethanol series, and embedded in Spurr's resin.<sup>40</sup> During embedding, careful attention was paid to orientation, to ensure that the joint would be sectioned in a lateral to medial plane (Figure 3).

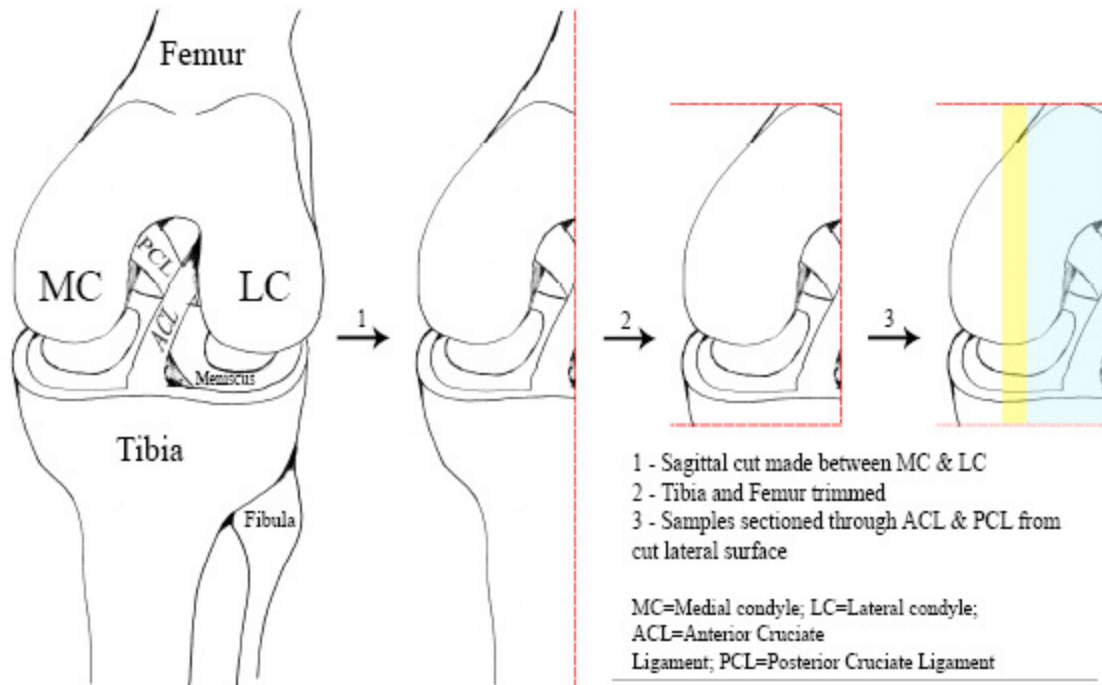


**Figure 3: Schematic Diagram of a left knee joint** showing how samples were trimmed and sectioned. blue = light sectioned yellow = TEM sectioned

### Light and Electron Microscopy

When polymerization was complete, each sample was trimmed and sectioned with an ultramicrotome. Light sections were cut 1000 nm thick and stained with 1% toluidine blue and azure II. Sections were viewed and photographed using an Olympus light microscope and RT Spot camera respectively (Diagnostic Instruments). Light sections were collected for orientation purposes and cell and matrix area fraction studies.

To ensure that transmission electron microscopy (TEM) samples did not vary significantly in depth for analysis, sections for electron microscopy were collected only after each sample had been light sectioned 42  $\mu\text{m}$  beyond the cruciate ligament. Samples in the 0 months age-group were too small to section 42  $\mu\text{m}$ , so samples were only sectioned until the full femoral head was visible. After sectioning for light microscopy, the blocks were trimmed to a small trapezoid for TEM (Figure 4). TEM sections were

cut 80 nm thin, transferred onto copper, carbon and formvar-coated grids, and post-stained with Reynold's lead citrate.<sup>41</sup> Ultra-thin sections were examined using an FEI T12 TEM and photographed using a Gatan MultiScan 794 digital camera at 1650X. TEM survey photos were collected using film photography because a greater area can be photographed than with digital photography.

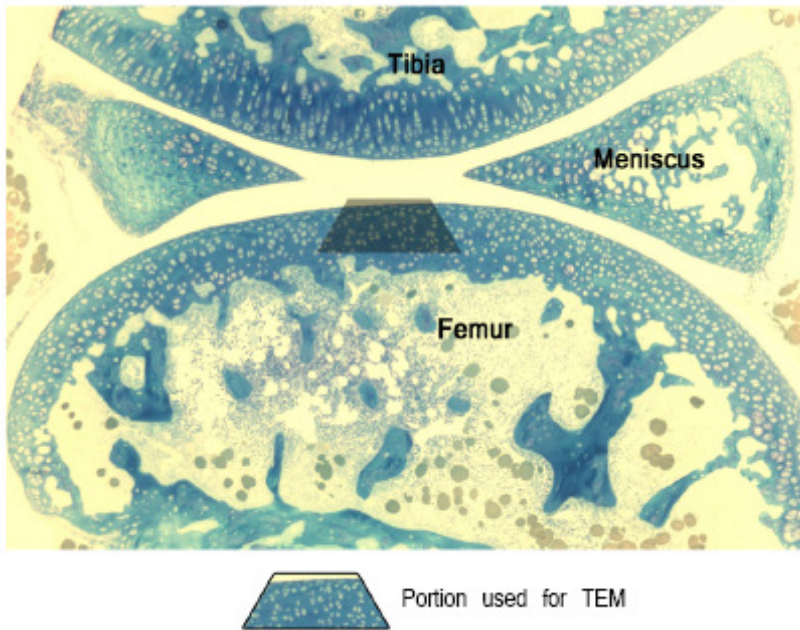


**Figure 4: Light micrograph of the knee joint** indicating how samples were trimmed for TEM

## Microscopic Analysis

### *ER Area Fraction*

Between 40-100 cells from each sample were randomly marked and photographed (Figure 5A) using the TEM for ER area fractions. Cells were divided into superficial and middle depths for data collection. (Data was not collected from cells in the calcified layer.) Both depths may have included some cells from the transitional layer because no visible delineation was observed between cartilage layers. The ER of each cell was traced using Image J (National Institutes of Health) scientific analysis program (Figure 5B). Threshold values were then adjusted so that Image J would automatically recognize

and measure each traced portion (Figure 5C); areas were recorded in  $\mu\text{m}^2$ . Total cell and nucleus areas were determined in the same manner. Using Microsoft Excel, the nucleus area was subtracted from the total cell area to determine the area of cytoplasm. Total ER area for each sample was divided by the cytoplasmic area and multiplied by 100 to determine what percent of the cytoplasm was ER (ER area fraction of the cell). ER fractions were used because the same depth location of each cell could not be guaranteed.

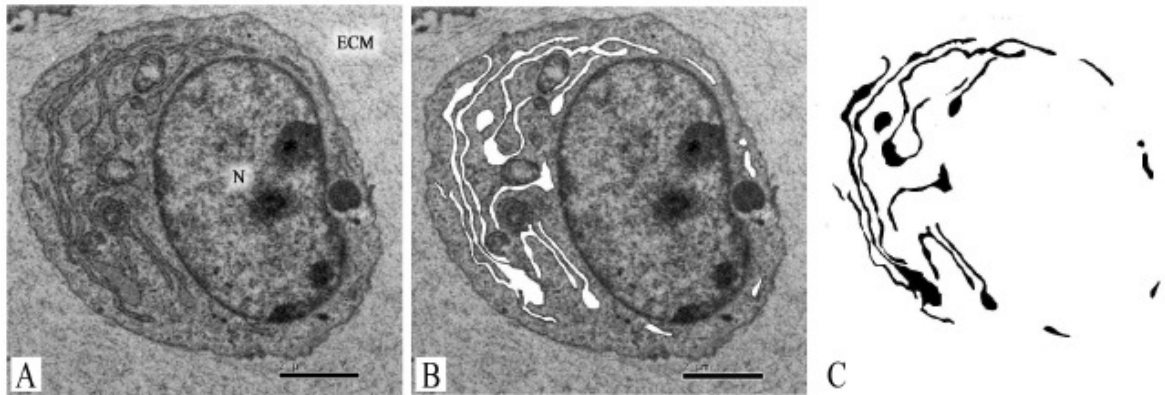


**Figure 5: Diagram illustrating ER area fraction analysis** and how the area of different cellular components was determined. **A)** TEM of a chondrocyte. **B)** TEM with ER traced using Image J. **C)** Threshold adjusted photo showing individual particles recognized and measured by Image J. N=nucleus ECM = matrix  $\mu\text{m}$  bar =  $2 \mu\text{m}$

### *Cell and Matrix Area Fractions*

Light micrographs for each sample were photographed using a Spot RT Color Camera (Diagnostic Instruments). An area  $158\mu\text{m}$  long and  $72\mu\text{m}$  wide was selected on each photo and used to determine cell and matrix area fractions (Figure 6A). Each photo was darkened so that cells would be more visible (Figure 6B). Cells in each photograph were traced as described previously, and the traced areas were threshold adjusted (Figure 6C). Image J automatically measured and recorded cell area fractions (total area occupied by cells). Any or all parts of cells visible in the light micrographs were

included in the cell fraction. Matrix area fraction was determined by subtracting cell area fractions from 100.

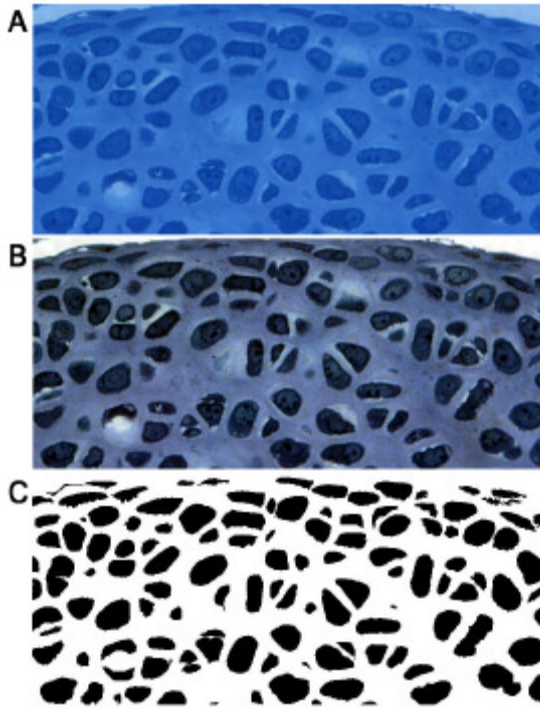


**Figure 6: Diagram illustrating how cell and matrix area fractions were determined** A) Area size used for measurement (158 $\mu\text{m}$ X72 $\mu\text{m}$ ). B) Darkened micrograph for tracing. C) Threshold adjusted micrograph measured by Image J.

### *Apoptosis*

Samples taken at 0.75 months and 7 months were viewed with the TEM at 1850X. Three random sections and areas were chosen for each sample and the number of cells in the visual field was counted for a total of six replicates. All cells that could possibly be dying were marked and viewed as digital micrographs to look for signs of apoptosis: cell shrinkage, condensed chromatin, and membrane blebbing. The number of cells that met these criteria

was recorded.

### **Statistical Analysis**

A three way repeated measures analysis of variance (ANOVA) was used to determine if mean ER area fractions were significantly different across age, genotype, and depth. Significance of cell and matrix area fractions across genotype and age was determined through a two way repeated measures ANOVA. In addition to standard p-values, a Tukey adjusted p-value is listed. The Tukey p-value is a conservative adjustment that reduces the chance of error. To increase sample size, +/- data from 7 and



9 month old animals was pooled; D/+ data from 7 and 9 month age groups was also pooled. Before pooling it was previously determined that data from both age groups were not statistically significant ( $p > .99$ ). The pooled age group will be referred to as 7 months for the remainder of the study. All statistical analysis was conducted using SAS © 9.1, SAS Institute Inc., Cary, NC, USA.

## RESULTS

### Cell and Matrix Area Fractions

#### *Genotype comparison for all ages*

Data from all age groups were pooled to compare differences across genotype only. The +/+ animals (ages combined) had an average cell fraction of 23.3% and average matrix fraction of 76.8%. Compared to these percentages, the D/+ had a higher cell and lower matrix area fraction by 6.5% (Figure 7)  $p < .004$  (Table 1). Light micrographs of articular cartilage stained with toluidine blue (Figure 8) and low magnification (survey) TEMs display this difference visually (Figure 9).

Table 1			
Area Fraction Comparison by Genotype (Ages Combined)			
Genotype Comparison		% Difference	p-value
+/+	D/+	6.51	0.0037

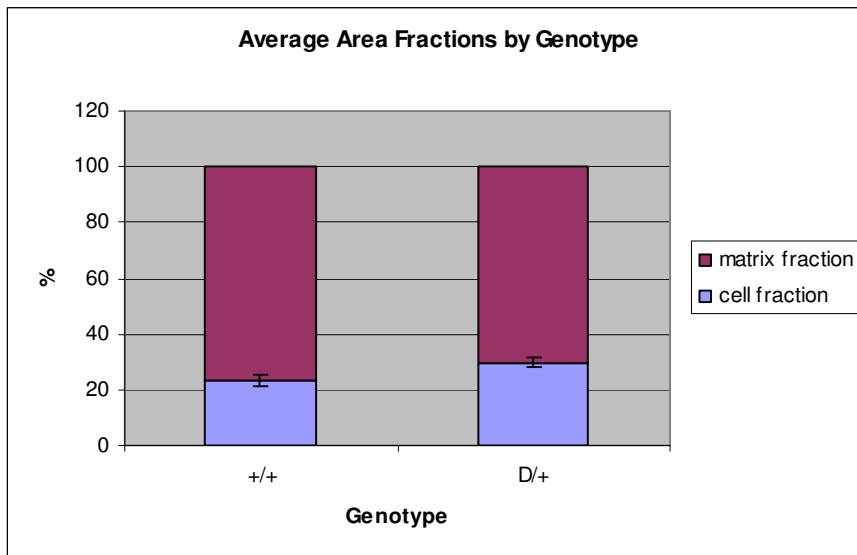


**Figure 7: Area fractions by genotype** show higher cell area fractions and a lower matrix area fractions in the D/+ compared to controls (all ages pooled)

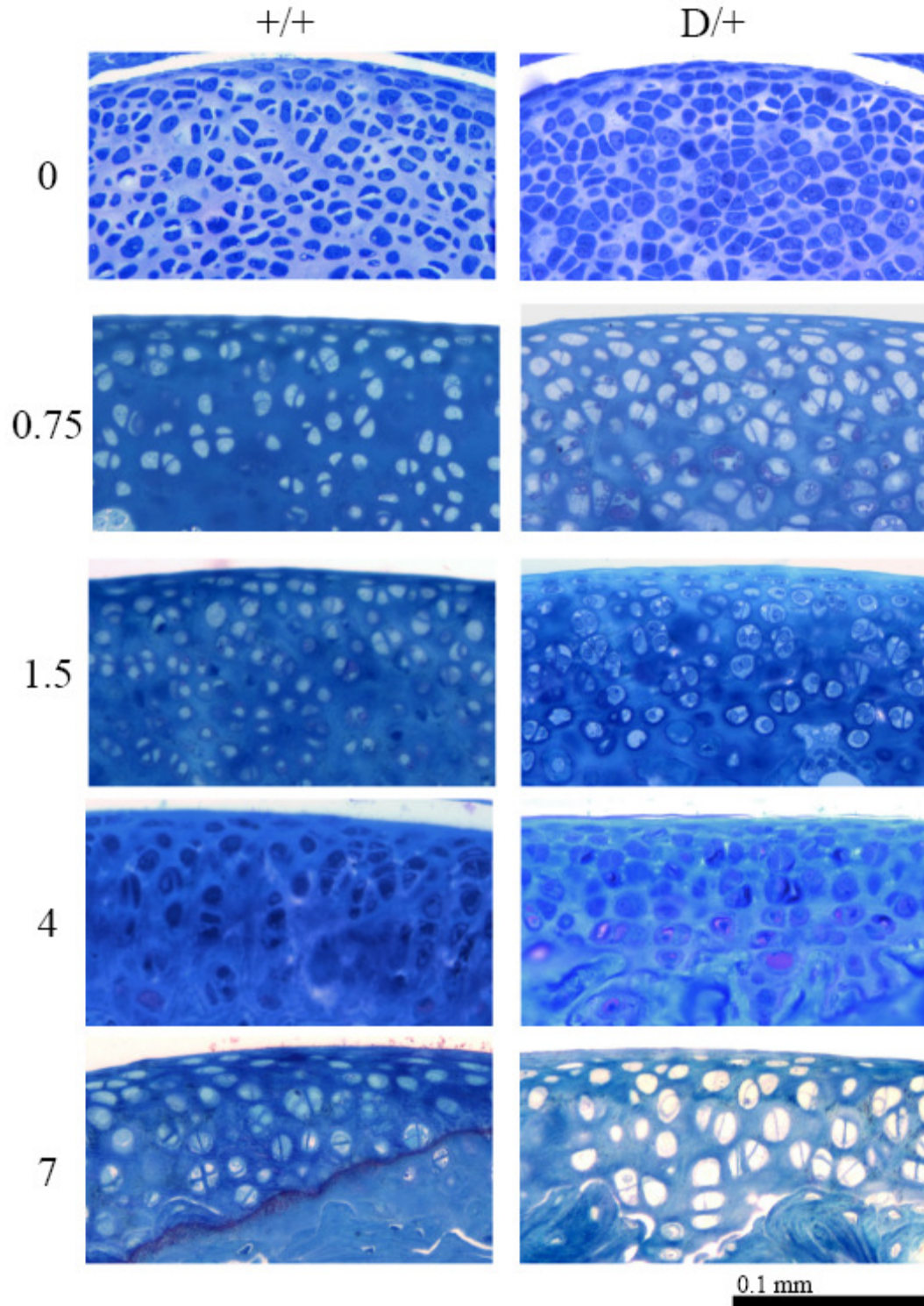


**Figure 8: Light micrographs of articular cartilage at all ages** (indicated at far left) stained with toluidine blue. D/+ mice have a visibly higher cell and lower matrix fraction. Cells appear larger in D/+ mice compared to +/+ mice.

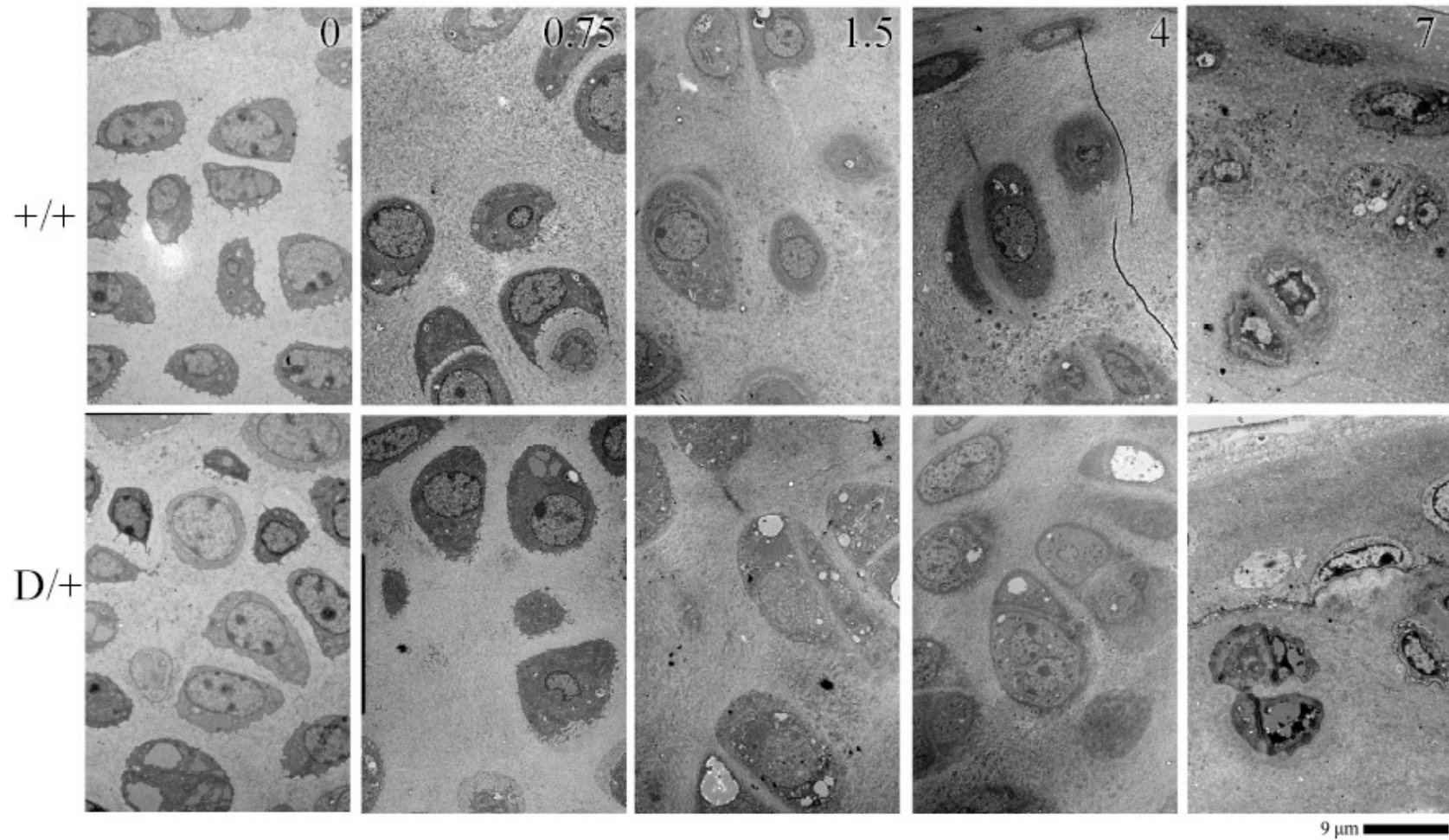


**Figure 9: Transmission electron micrographs for all ages** (indicated at top right). At 0 months cells are larger and matrix fraction appears lower in D/+ mice compared to +/+. At 1.5 months more lipids and degenerating mitochondria are visible. At 7 months more necrotic cells are visible. Collagen fibrils appear normally distributed in all ages and genotypes.

### *Genotype comparison within ages*

At zero months, the average cell fraction in +/+ mice was 35.2%, 43.35% in D/+ mice, and 42.44% in D/D mice. While both the homozygous mutant and the heterozygote showed a higher cell and lower matrix area fraction compared to the +/+ (Figure 10, Figure 11) the comparisons between each genotype showed no significant differences (Table 2). Visual differences were apparent in the matrix composition at 0 months (Figure 15).

In +/+ animals at 0.75 months, the cell and matrix fractions were 22.4% and 77.6% respectively. D/+ animals had a higher cell fraction (34.4%) (Figure 10) and lower matrix fraction (65.6%) (Figure 11) compared to the age-matched controls (12% difference). Unadjusted, the difference is shown to be significant ( $p=0.018$ ), and with the conservative Tukey adjustment, no significance is demonstrated ( $p=0.26$ ) (Table 2).

In +/+ animals at 1.5 months, the cell and matrix fractions were 24.25% and 75.75% respectively. D/+ animals had a higher cell fraction (29.35%) (Figure 10) and lower matrix fraction (70.65%) (Figure 11) compared to the age-matched controls (5.1% difference). Unadjusted and adjusted p-values show no statistical significance ( $p=0.27$ ,  $p\text{-adj}=0.96$ ) (Table 2).

In +/+ animals at 4 months, the cell and matrix fractions were 17.03% and 82.97% respectively. D/+ animals had a higher cell fraction (21%) (Figure 10) and lower matrix fraction (79%) (Figure 11) compared to the age-matched controls (3.97% difference). Unadjusted and adjusted, p-values show no statistical significance ( $p=0.29$ ,  $p\text{-adj}=0.97$ ) (Table 2).

In +/+ animals at 7 months, the cell and matrix fractions were 20.2% and 79.8% respectively. D/+ animals had a higher cell fraction (24.8%) (Figure 10) and lower matrix fraction (75.2%) (Figure 11) compared to the age-matched controls (4.6% difference). Unadjusted and adjusted, p-values show no statistical significance (p=.31, p-adj=.98) (Table 2).

All D/+ animals show higher cell area fractions and lower matrix area fractions consistently in each age group. Within age groups, statistical significance could not be demonstrated for differences except at 0.75 months, but it should be noted that a trend exists. The ER fractions data with all ages combined does in fact show a significant difference (p<.004).

Table 2						
Area Fraction Comparisons by Genotype within Ages						
Age (months)	Genotype Comparison		Cell Fraction % Difference	Matrix Fraction % Difference	p-value	Tukey p-value
0	+/+	D/+	-8.15	8.15	0.086	.69
	+/+	D/D	-7.24	7.24	0.20	0.37
	D/+	D/D	0.91	-0.91	0.85	0.98
0.75	+/+	D/+	-10.4	10.4	<b>0.018</b>	0.25
1.5	+/+	D/+	-5.1	5.1	0.27	0.96
4	+/+	D/+	-3.97	3.97	0.29	0.97
7	+/+	D/+	-4.6	4.6	0.31	0.98

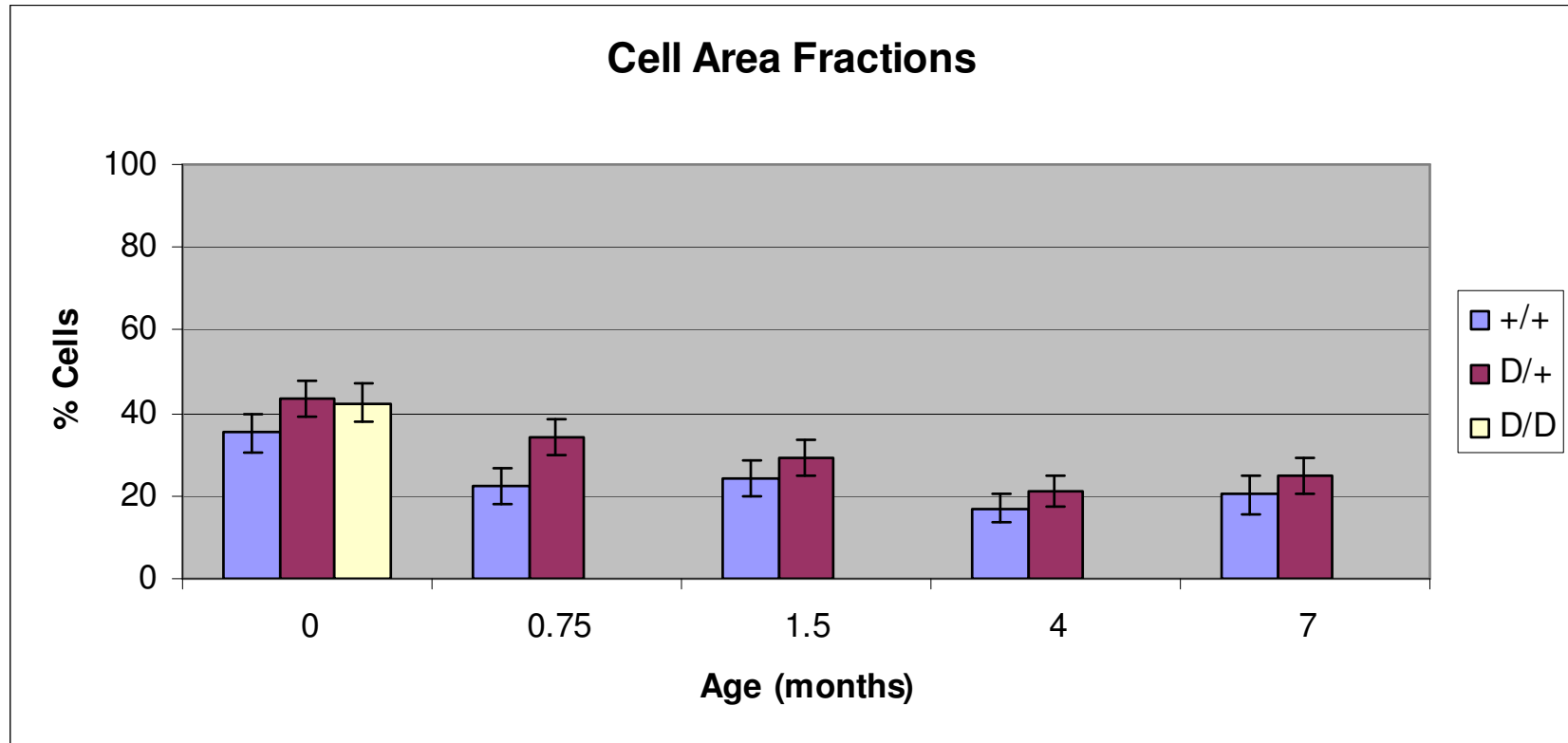


**Figure 10: Bar graphs for cell area fractions at each age**

At 0.75 months, D/+ mice have a significantly higher cell fraction compared to +/+ mice.

No significant differences in cell area fractions were observed between +/+, D/+, or D/D mice at any other age.

Cell fractions were always higher in D/+ animals.

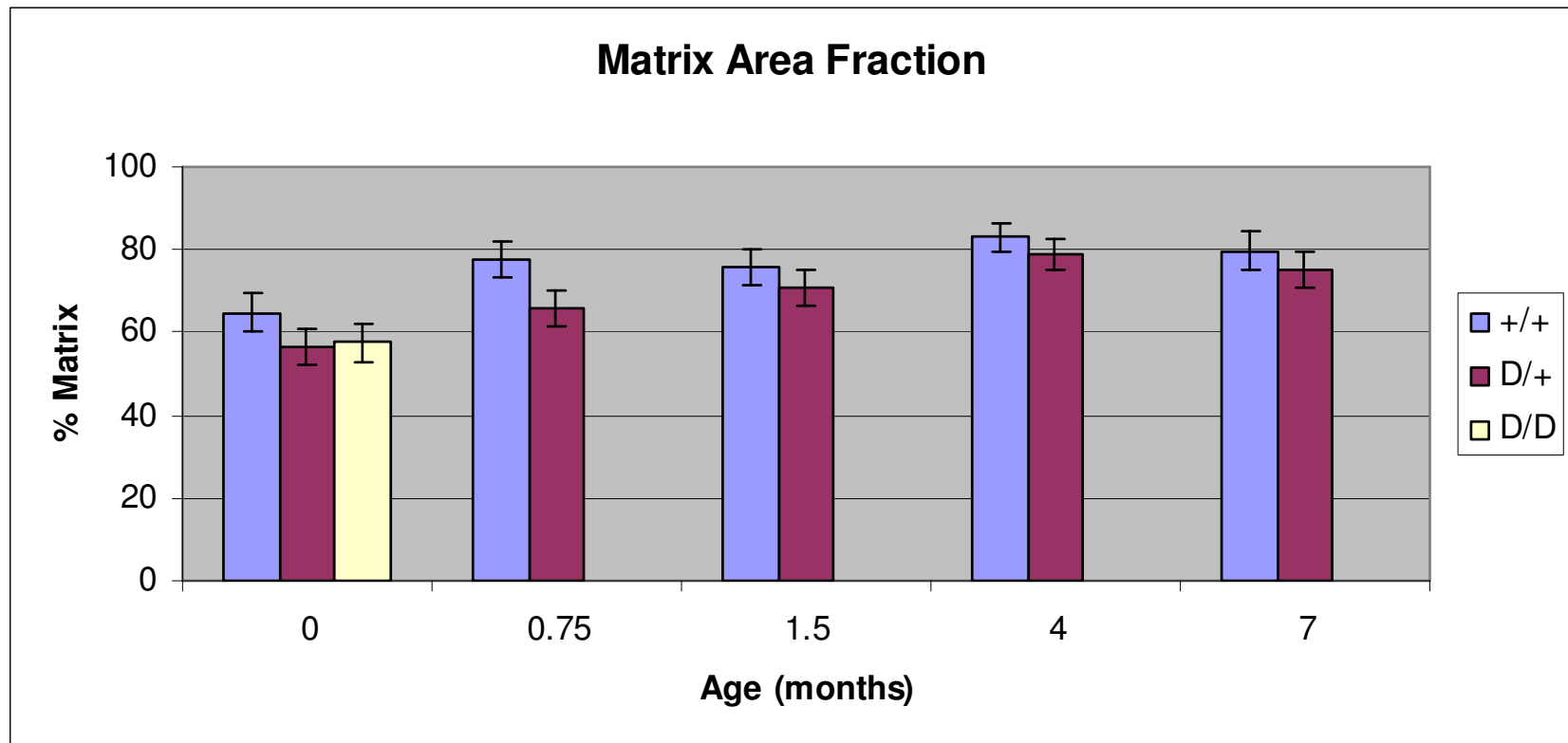


**Figure 11: Bar graphs of matrix area fractions at each age**

At 0.75 months, D/+ mice have a significantly lower matrix fraction compared to +/+ mice.

No significant differences in matrix area fractions were observed between +/+, D/+, or D/D mice at any other age.

Matrix fractions were always lower in D/+ animals.



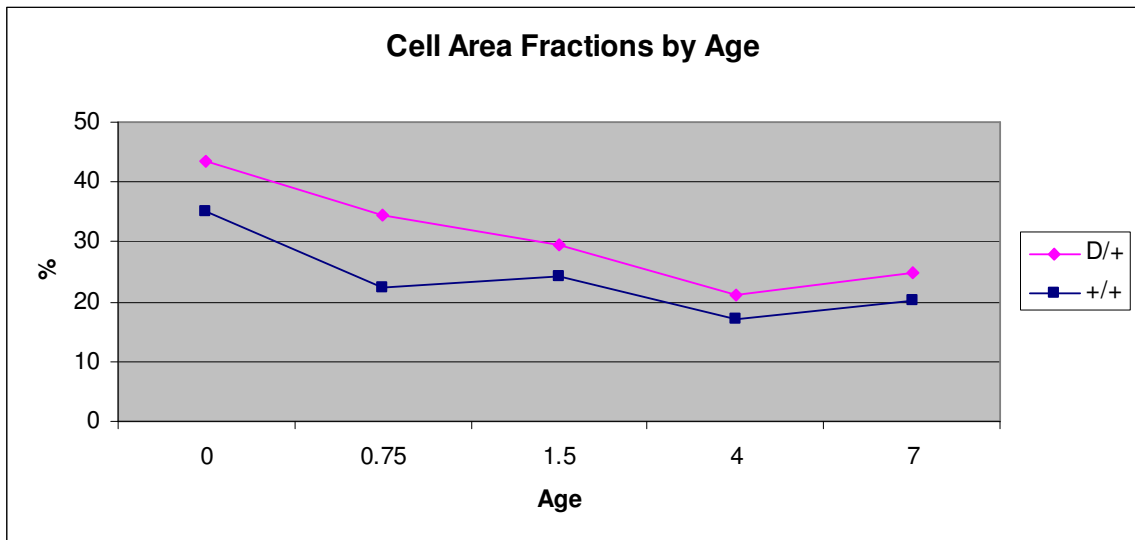
*Age comparison within genotypes*

Cell and matrix area fractions were also compared within genotypes at various ages. In +/+ animals, most of the differences were not significant. Cell and matrix area fractions in the +/+ animal at 0 months, however, were significantly different from all other ages in the +/+ genotype (Table 3). In the D/+, most of the significant differences were seen in the 0 days age group. Cell and matrix area fractions in ages 1.5, 4, and 7 months were found to be significantly different from fractions at 0 months (Table 4, Figure 12, Figure 13). Cell and matrix area fractions from D/+ mice 4 and 7 months old were also significantly different from fractions of D/+ mice 0.75 months old (Table 4). No significant difference was observed in cell and matrix area fractions between the D/+, 0 month and 0.75 months animals (Table 4).

A consistent trend is seen in the cell and matrix fractions as the animals age. The +/+ cell fraction is always lower and the matrix fraction is always higher than D/+ mice, and with age the cell fraction consistently decreases and the matrix fraction increases irrespective of genotype (Figure 12, Figure 13).

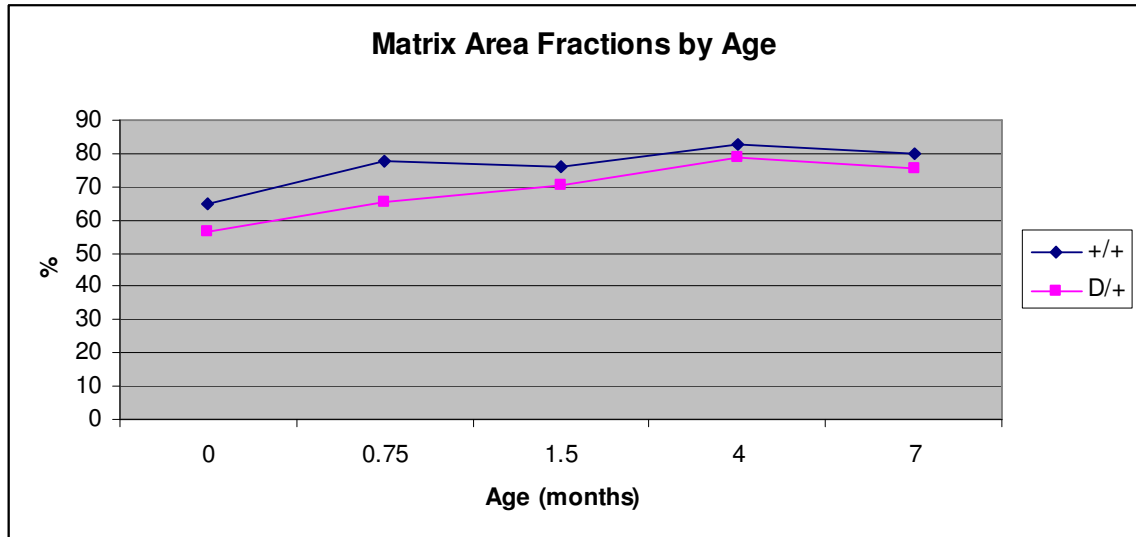
<b>Table 3</b>					
Area Fraction Comparisons in +/+ Mice across Ages					
Genotype	Compared Ages(months)	% Difference	p-value	Tukey p-value	
+/+	0	0.75	12.8	0.013	0.20
		1.5	10.95	0.028	0.35
		4	18.17	0.0007	0.015
		7	15	0.0049	0.091
	0.75	1.5	-1.85	0.68	1
		4	5.37	0.20	0.92
		7	2.2	0.62	1
	1.5	4	7.22	0.095	0.72
		7	4.05	0.37	0.99
	4	7	-3.17	0.44	1

Table 4					
Area Fraction Comparisons in D/+ Mice across Ages					
Genotype	Compared Ages(months)		% Difference	p-value	Tukey p-value
D/+	0	0.75	8.95	0.06	0.59
		1.5	14	0.0075	0.13
		4	22.35	0.0001	0.0029
		7	18.55	0.0011	0.025
	0.75	1.5	5.05	0.27	0.97
		4	13.4	0.0056	0.10
		7	9.6	0.048	0.50
	1.5	4	8.35	0.058	0.56
		7	4.55	0.32	0.98
	4	7	-3.8	0.36	0.99



**Figure 12: Cell area fraction comparison over time**

Over time the cell fraction decreases in +/+ and D/+ mice, and the difference between them becomes smaller.



**Figure 13: Matrix area fraction comparison over time**  
 Over time the matrix fraction increases in both the +/+ and D/+ mice, and the difference between them becomes smaller.

### ER Area Fraction

Initially the focus of the ER study was to be in animals at ages 6 and 9 months. Upon completion of preliminary data, it was discovered that the ER dilation previously documented in other osteoarthritis models<sup>32</sup> was not pronounced in animals examined at 7 and 9 months old. An observable difference was seen at 4 months, so it was determined that animals younger than 4 months should be included in the study. For this reason, ages explored extensively include 0, 0.75, 1.5, 4, and 7 months. Furthermore, it is well established that cells in different zones of articular cartilage are morphologically distinct,<sup>2</sup> so results are included that show ER area fractions at different depths (superficial and middle) in articular cartilage.

#### *Genotype comparison for all ages*

Data from the 0.75, 1.5, 4, and 7 months age groups were pooled to compare differences across genotype only (Figure 14). The cells from +/+ mice (ages combined) had an average ER fraction of 8.86% (depths combined). In +/+ animals, superficial cells

had an average ER fraction of 8.18%, and in middle cells, 9.82%. In D/+ mice, ER area fractions were significantly increased in middle cells (12.48%) and in the combined depth analysis (10.62%) (Table 5). No significant difference was detected between ER area fractions in superficial cells of +/+ and D/+ mice (Figure 14).

Table 5				
ER Area Fraction Comparison by Genotype (Ages Combined)				
Depth	Genotype Comparison		% Difference	p-value
Both	+/+	D/+	1.77	0.0022
Superficial			1.26	0.13
Middle			2.66	0.0013

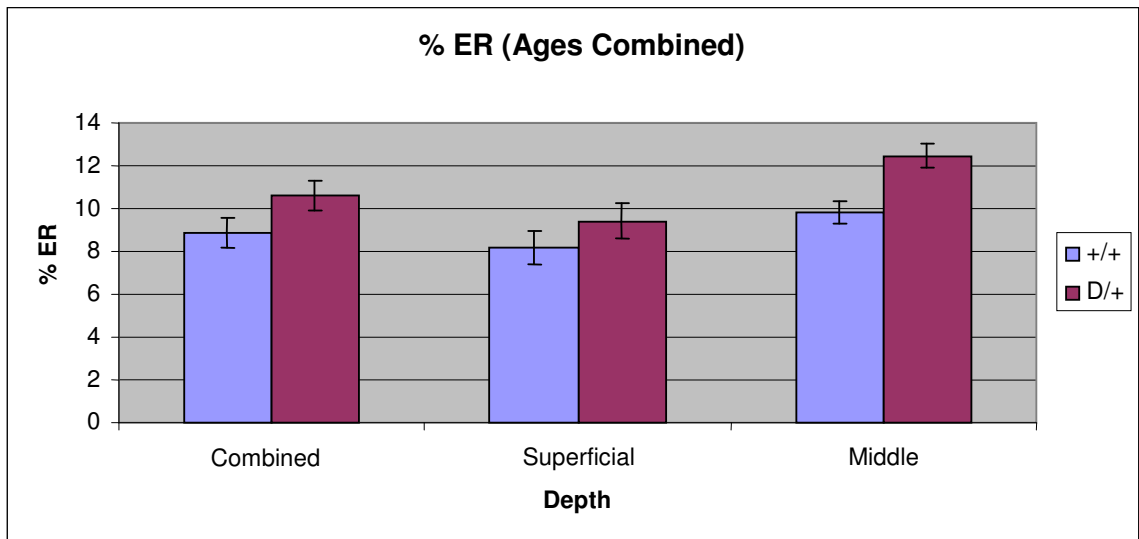


**Figure 14: Bar graphs of ER fractions (ages combined)**

D/+ animals show a significantly higher ER fraction compared to +/+ animals (ages combined) in middle cells and combined depths analysis.

*Genotype comparison within ages*

In combined depths at 0 months, the mean ER fraction for +/+ mice was 12.2%, 15.93% for D/+ mice, and 27.93% for D/D mice. The ER fraction of D/D mice was significantly higher than the +/+ (p=.008) and the D/+ (p=.017), displaying that the ER is in fact dilated in D/D animals. The data also show that the aforementioned differences are more pronounced in superficial cells, and barely significant in middle cells. The +/+ and D/+ mice had ER fractions that were significantly different from each other in middle cells (p=.011) and combined depths analysis (p=.0028) (Table 6, Figure 15, Figure 16, Figure 17)

<b>Table 6</b>					
ER Area Fraction Comparisons by Genotype at 0 Months					
Depth	Genotype Comparison		% Difference	p-value	Tukey p-value
Combined	<b>+/+</b>	<b>D/+</b>	<b>3.73</b>	<b>0.011</b>	<b>0.18</b>
	+/+	D/D	15.73	0.0081	0.016
	D/+	D/D	12.01	0.017	0.035
Superficial	<b>+/+</b>	<b>D/+</b>	<b>1.51</b>	<b>0.42</b>	<b>1</b>
	+/+	D/D	14.86	0.0069	0.014
	D/+	D/D	13.34	0.0093	0.019
Middle	<b>+/+</b>	<b>D/+</b>	<b>5.94</b>	<b>0.0028</b>	<b>0.056</b>
	+/+	D/D	16.61	0.045	0.089
	D/+	D/D	10.67	0.12	0.23

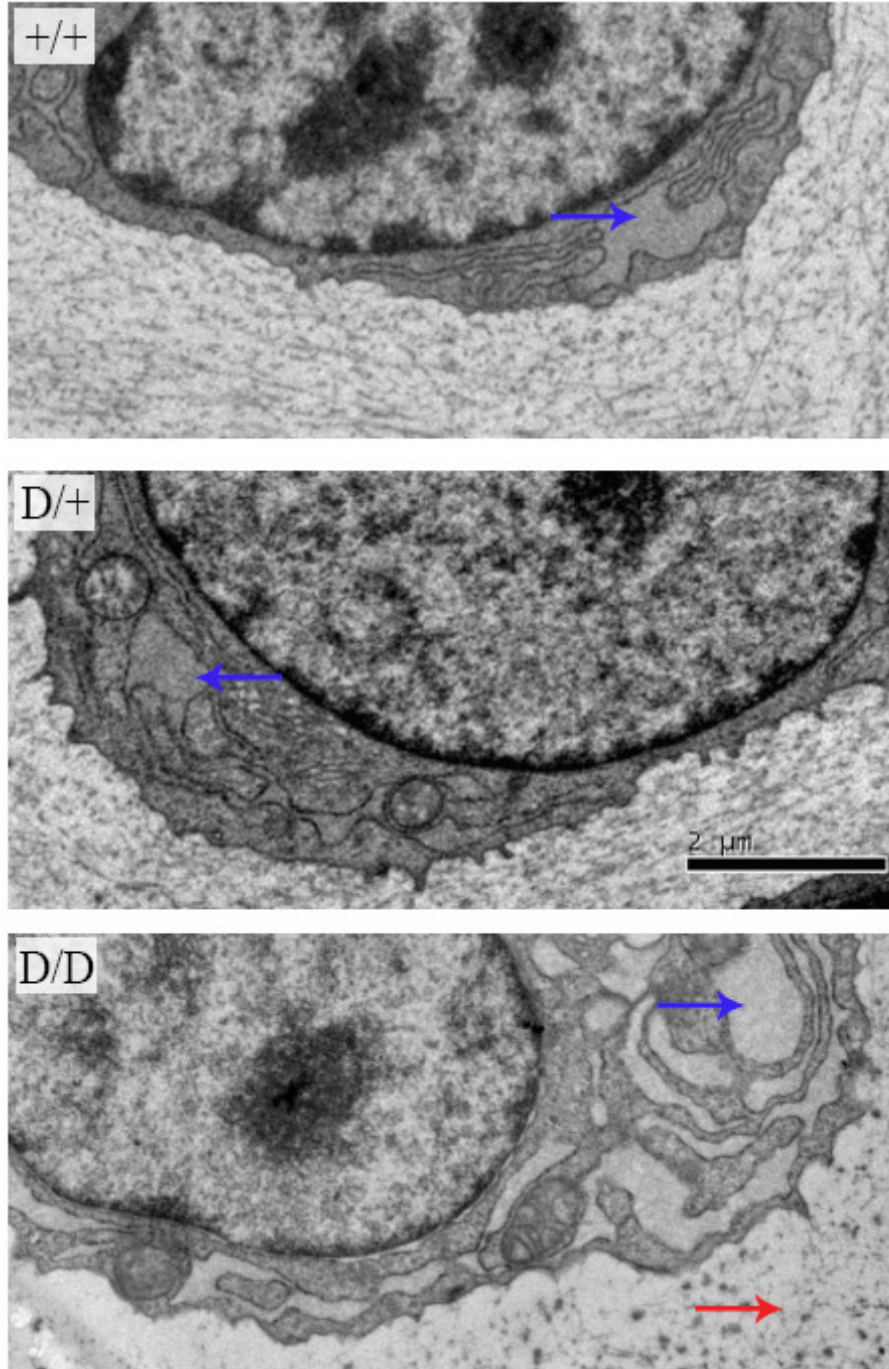


**Figure 15: Matrix and ER TEM at 0 months.**

Red arrow points to decreased collagen fibrils and organization in D/D mice. Blue arrows show dilation in the ER. In D/D mice this dilation is significant and has a fibrous appearance.

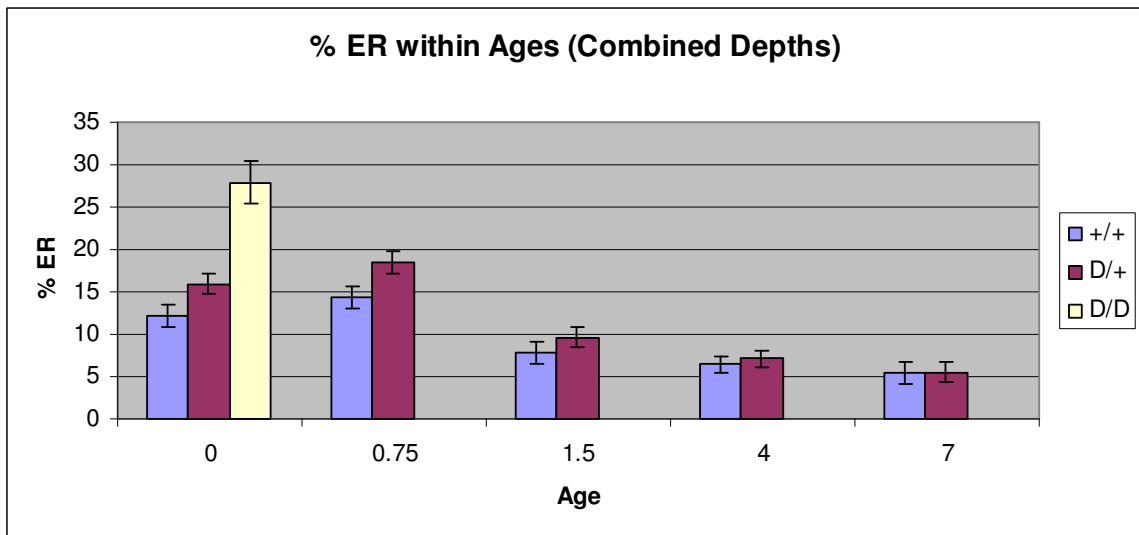


**Figure 16: ER Area Fractions for all ages (depths combined)**  
 ER fractions in D/+ mice are higher and significantly different than +/+ mice at 0 and 0.75 months. ER fractions in +/+ and D/+ mice peak at 0.75 months and subsequently decrease.

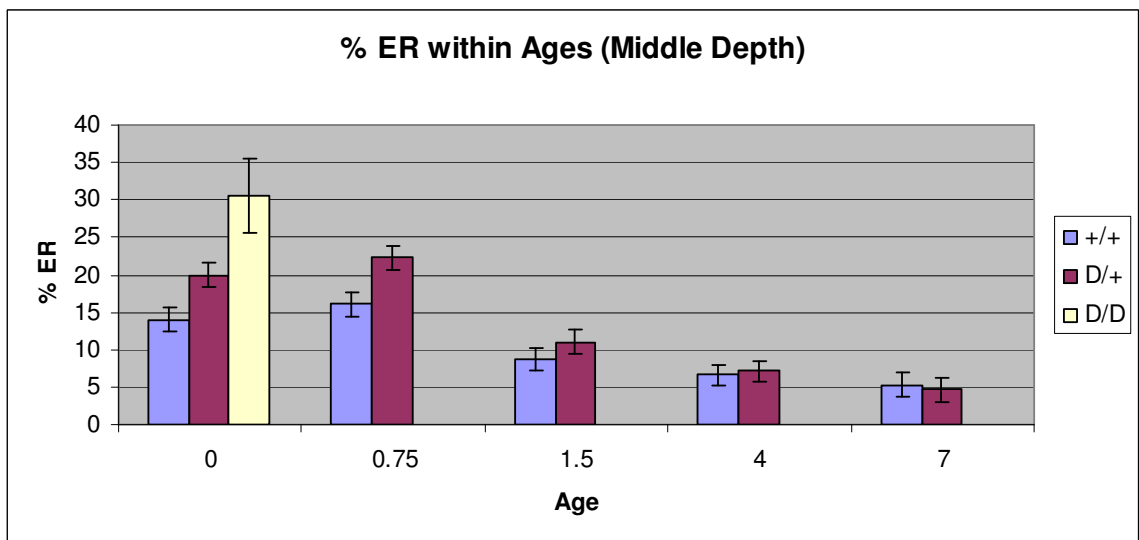


**Figure 17: Bar graphs of ER fractions at all ages in middle cells**  
 ER fractions in D/+ mice are higher and significantly different than +/+ mice at 0 and 0.75 months in middle cells. ER fractions in +/+ and D/+ mice peak at 0.75 months and subsequently decrease. In middle cells, the ER fraction of D/+ mice drops below the +/+ fraction at 7 months.

Significant differences were seen in the ER fractions between +/+ and D/+ mice at 0 and 0.75 months (ages combined) (Table 7) in combined depths (Figure 16) and middle cells (Figure 17). No significant differences between +/+ and D/+ mice were observed at any age in the superficial cell group (data not included). Furthermore, no significant differences were seen between the +/+ and D/+ at 1.5, 4, or 7 months (Table 7) in combined (Figure 16) or middle (Figure 17) ER fractions (Figure 19, Figure 20, Figure 21). The D/+ mice do however have a consistently higher ER area fraction compared to +/+ mice in combined depths. The ER fraction is actually lower in D/+ mice compared to the +/+ (not statistically significant) at 7 months in middle cells (Table 7). In addition to a higher ER fraction, lipids and degenerating mitochondria were seen frequently in D/+ mice at 1.5 months, but not in +/+ mice (Figure 9). Lastly, intracellular filaments were observed more often in D/+ mice at 0.75 months and 1.5 months compared to +/+ animals (Figure 18, Figure 19).



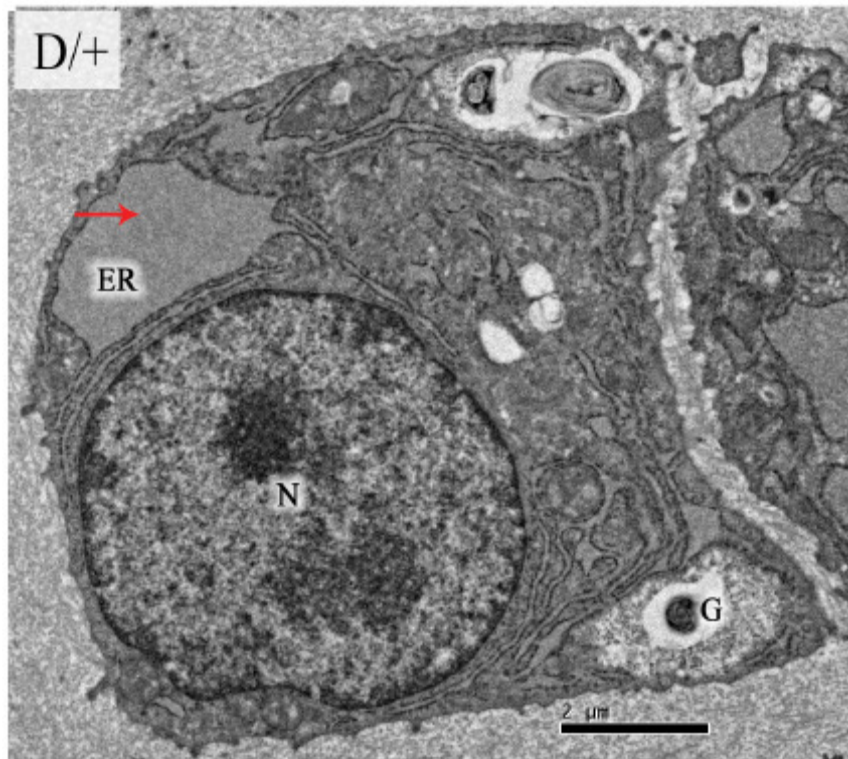
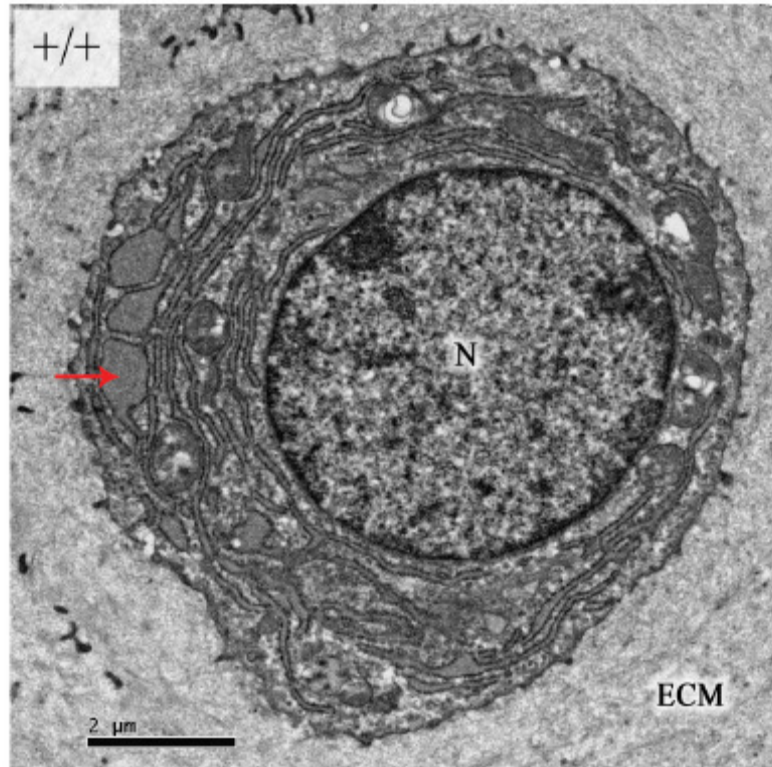


**Figure 18: TEM of middle chondrocytes at 0.75 months**  
Red arrows point to dilations in the ER. In D/+ mice this dilation is significant. N=nucleus, ECM= extracellular matrix, ER=endoplasmic reticulum, G=glycogen

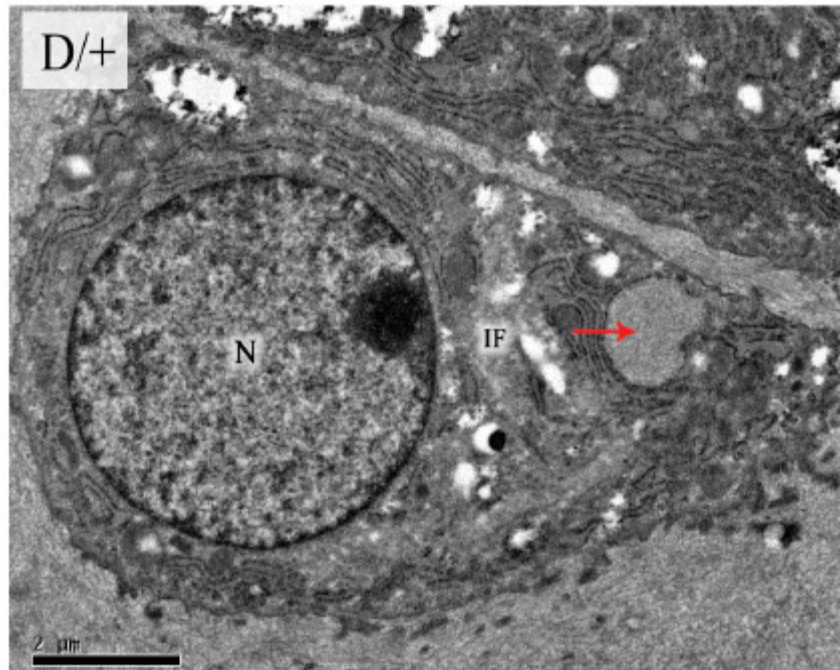
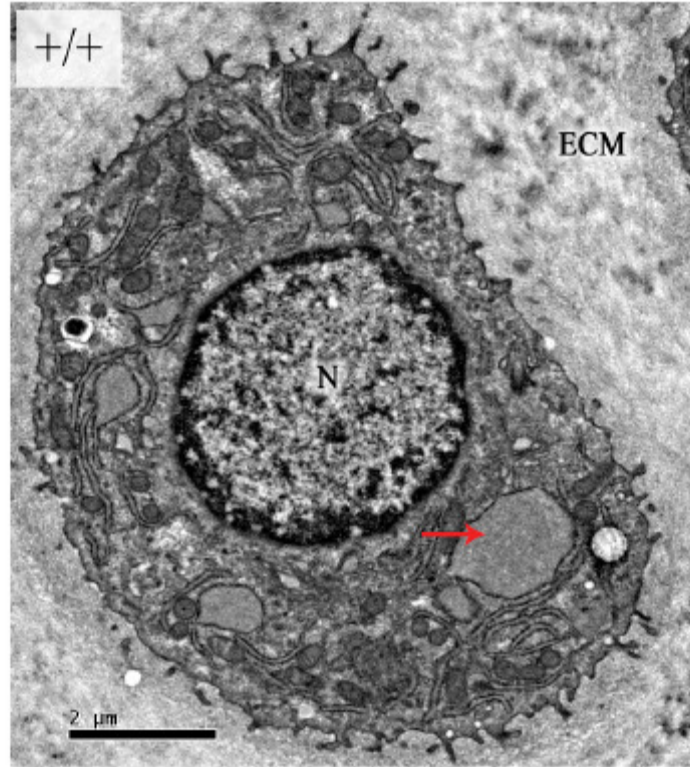


**Figure 19: TEM of middle chondrocytes at 1.5 months**  
+/+ and D/+ middle chondrocytes at 1.5 months show some dilation in the ER (red arrows), prominent intracellular filaments. N=nucleus, ECM=extracellular matrix, IF=intracellular filaments.

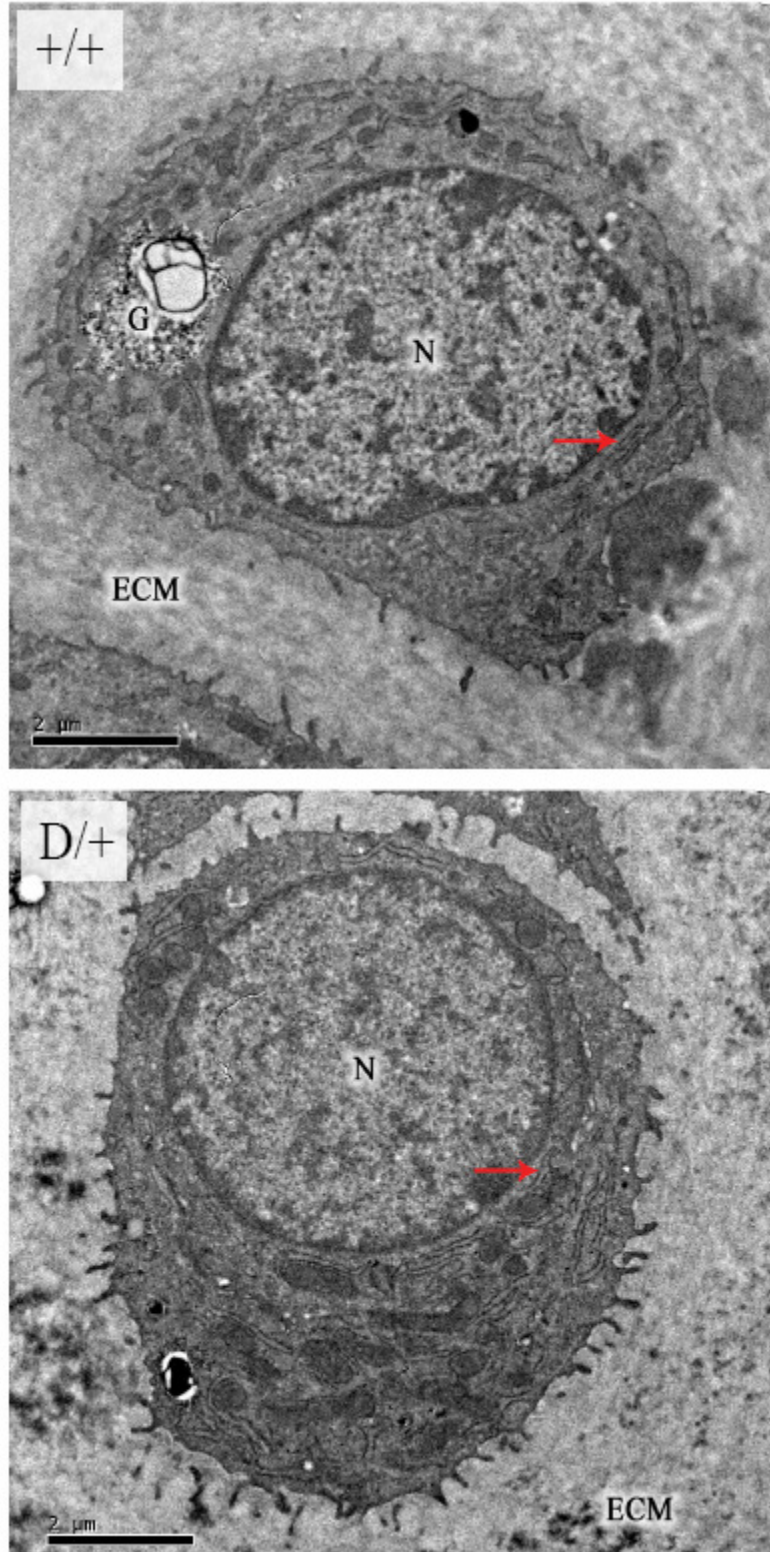


**Figure 20: TEM of middle chondrocytes at 4 months**

Middle chondrocytes from +/+ and D/+ mice at 4 months show a visible decrease in dilation of the ER (red arrows). N=nucleus, ECM=extracellular matrix

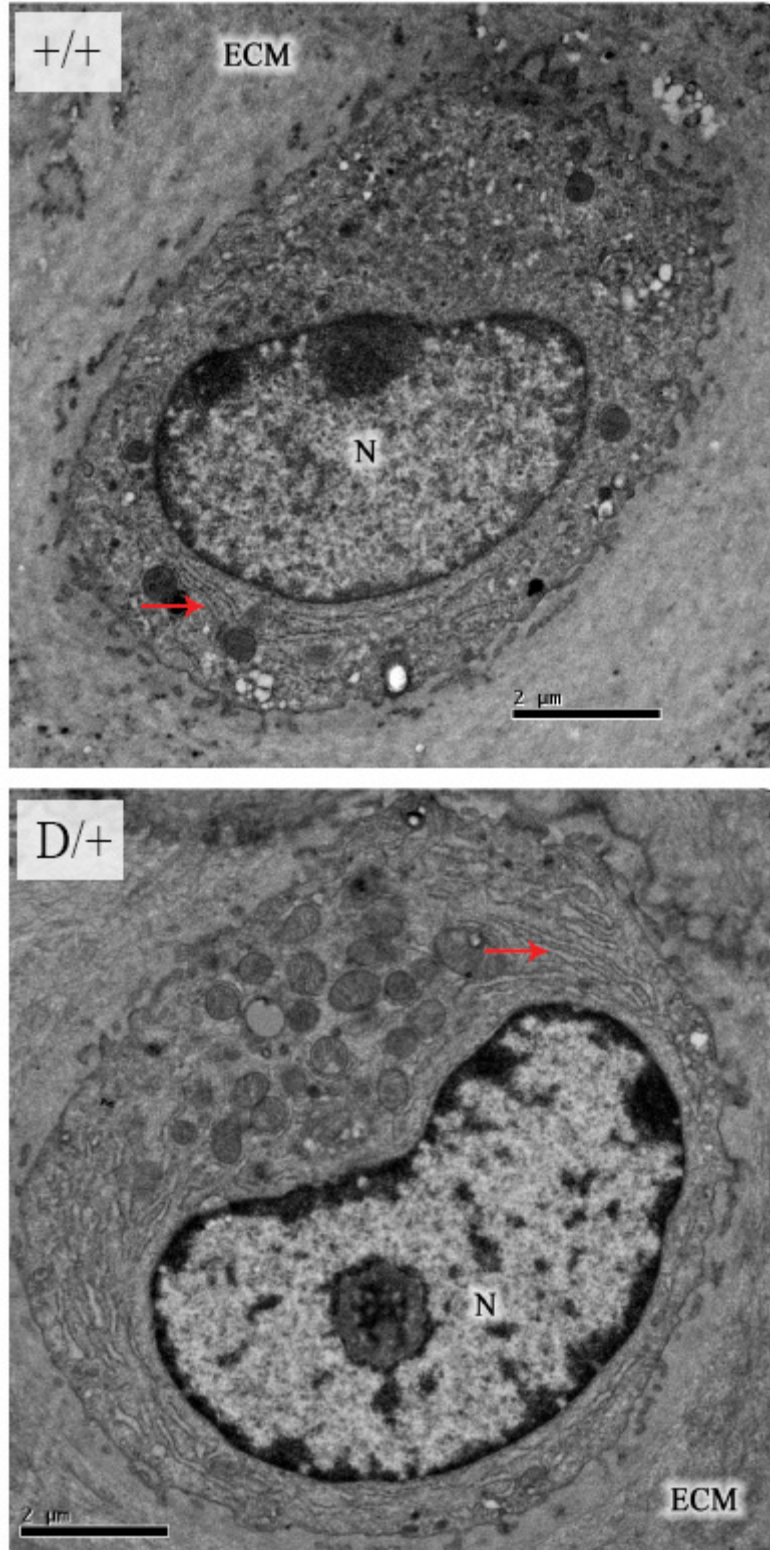


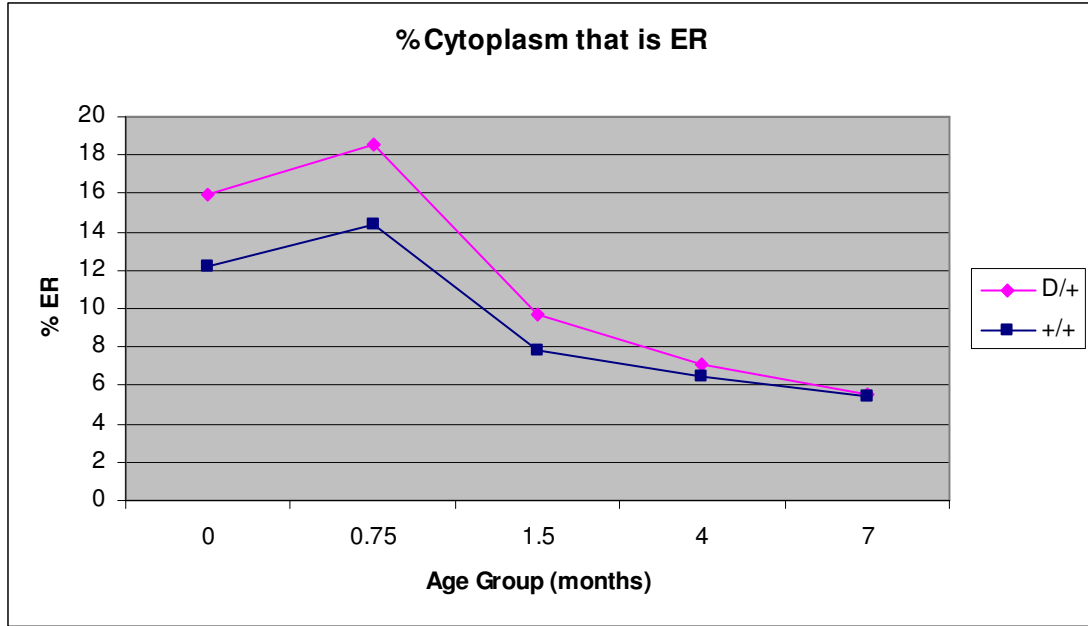
**Figure 21: TEM of middle chondrocytes at 7 months**

No obvious difference is observable between the ER of chondrocytes in +/+ or D/+ mice. Red arrows point to the ER. N=nucleus, ECM= extracellular matrix

Table 7					
ER Area Fraction Comparisons by Genotype within Ages					
Depth	Age (months)	Avg. %ER in +/+	Avg. %ER in D/+	p-value	Tukey p-value
Combined	0	12.20	15.93	0.011	0.18
	0.75	14.40	18.52	0.0063	0.11
	1.5	7.80	9.64	0.17	0.88
	4	6.42	7.10	0.52	1
	7	5.45	5.51	0.96	1
Superficial	0	10.39	11.90	0.42	1
	0.75	12.67	14.74	0.28	0.97
	1.5	6.93	8.25	0.48	1
	4	6.23	7.10	0.57	1
	7	5.63	6.33	0.71	1
Middle	0	14.01	19.95	0.0028	0.056
	0.75	16.12	22.30	0.0021	0.044
	1.5	8.67	11.02	0.16	0.88
	4	6.62	7.11	0.71	1
	7	5.27	4.68	0.72	1

#### *Age comparison within genotypes*

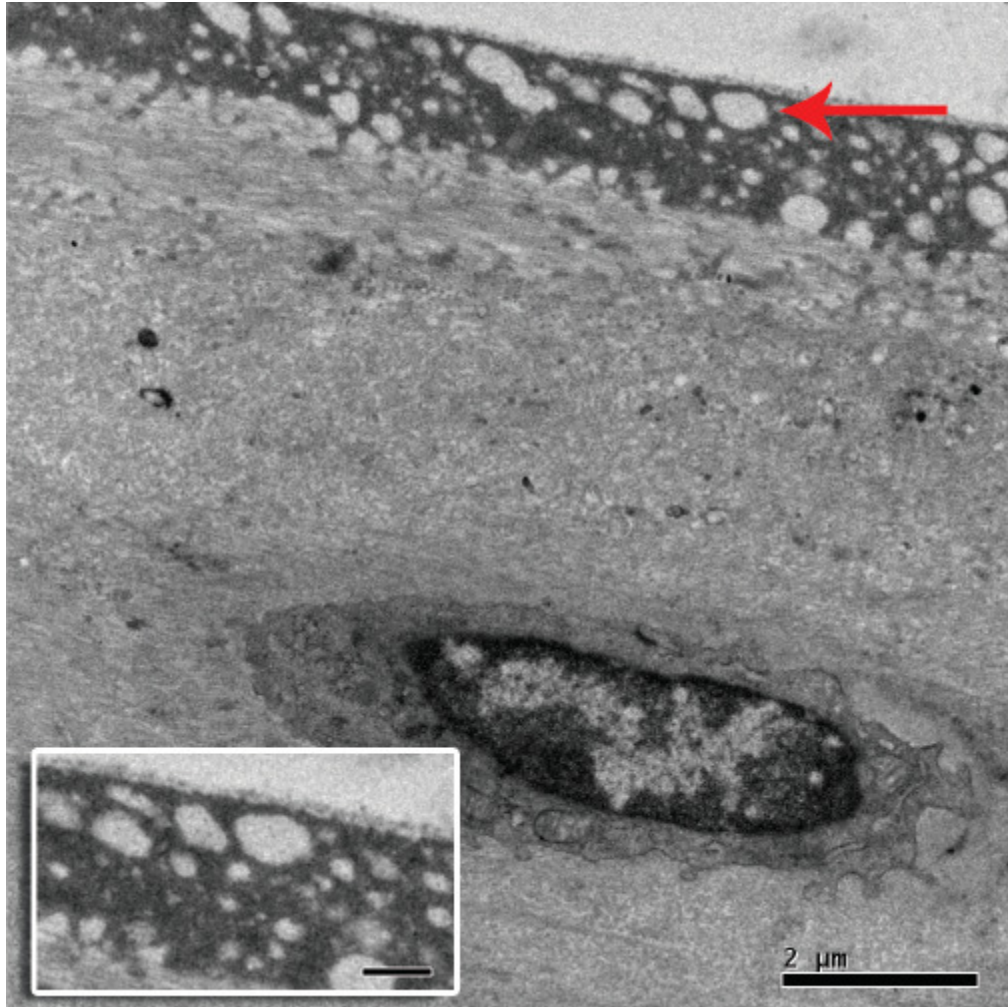
Within genotypes and across age groups, ER area fractions in animals from the 0 and 0.75 months ages were significantly higher in both genotypes compared to 1.5, 4, and 7 month old animals (Table 8). ER area fractions in animals at 0 and 0.75 months, however, were not significantly different from each other in either genotype group. At 1.5 months, ER fractions in the D/+ mice were significantly different from ER fractions in D/+ mice 4 (p=.046) and 7 (p=.0062) months old. The data also show a consistent trend. At 3 weeks, the % ER peaks in both genotypes, and progressively decreases, until the % ER values of +/+ and D/+ mice actually merge (Figure 22). Other qualitative observations include changes and lesions in the superficial zone (Figure 23, Figure 24).



**Figure 22: ER Area Fraction Changes with Age (depths combined)**

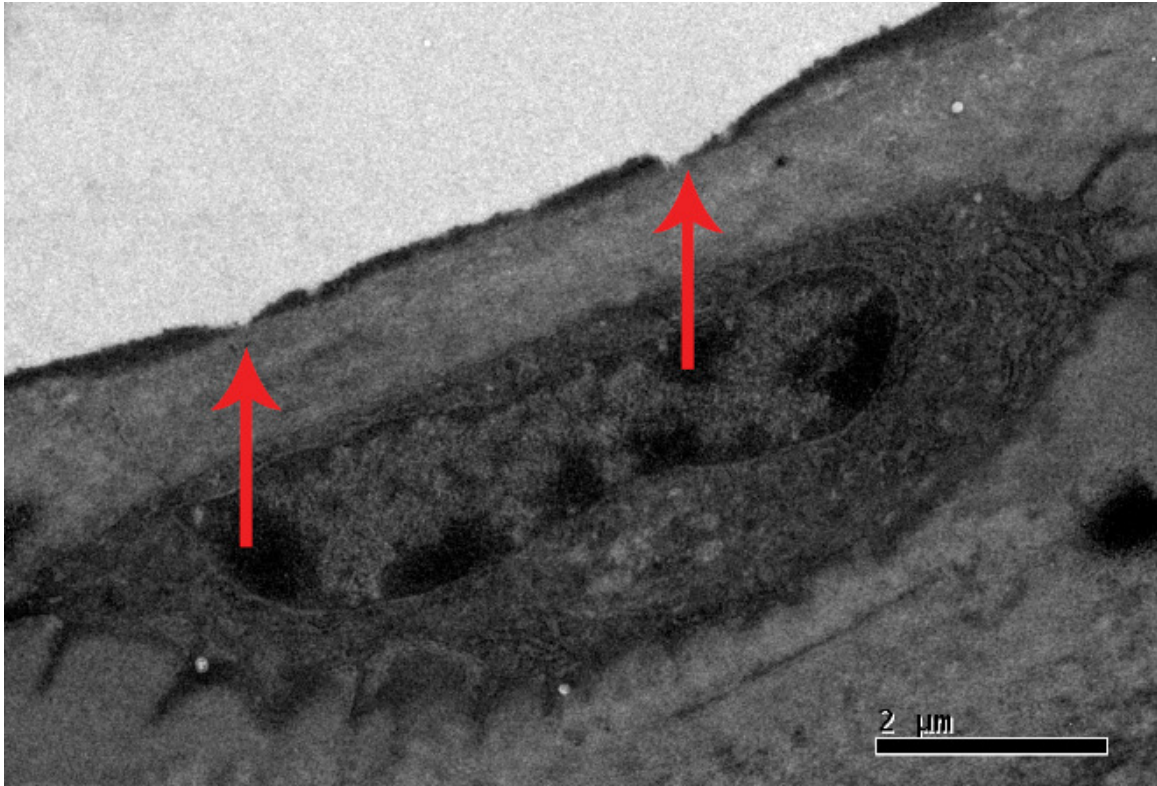
The ER fraction is higher in the D/+ at young ages, but as the D/+ animals age, the ER fraction difference from the +/+ becomes zero in combined depths.

Table 8					
ER Area Fraction Comparisons within Genotypes and across Ages (depths combined)					
Genotype	Compared Ages(months)		% Difference	p-value	Tukey p-value
+/+	0	0.75	-2.20	0.10	0.75
		1.5	4.40	0.0042	0.079
		4	5.78	0.0003	0.0067
		7	6.75	0.0002	0.004
	0.75	1.5	6.60	0.0002	0.0048
		4	7.97	<.0001	0.0004
		7	8.95	<.0001	0.0003
	1.5	4	1.38	0.25	0.96
		7	2.35	0.084	0.68
	4	7	0.97	0.41	1
D/+	0	0.75	-2.59	0.060	0.57
		1.5	6.29	0.0003	0.007
		4	8.82	<.0001	0.0001
		7	10.42	<.0001	<.0001
	0.75	1.5	8.88	<.0001	0.0003
		4	11.42	<.0001	<.0001
		7	13.01	<.0001	<.0001
	1.5	4	2.53	0.046	0.49
		7	4.13	0.0062	0.11
	4	7	1.60	0.19	0.91



**Figure 23: TEM of Changes in the Superficial Matrix**

D/+ chondrocyte and surrounding matrix in articular cartilage at 9 months. Red arrow points to fibrillation and openings (water or increased permeability) in the most superficial layer. Inset at lower left corner (bar = 0.5 $\mu$ m) shows a larger view of these openings.



**Figure 24: Lesions in the Superficial Matrix**

Chondrocyte and surrounding matrix in articular cartilage at 4 months in D/+. Red arrows point to lesions in the most superficial layer.



## Apoptosis

Apoptosis was increased in both genotypes at older ages. Within age groups, however, no obvious differences in the number of dying cells were observed between the +/+ and D/+ mice (Table 9). In all cases, dying cells were only observed in the calcified zone of articular cartilage. All cells did have condensed chromatin (Figure 25). Some necrotic cells may have also been included in the counts. Statistical significance was not determined.

Age (months)	Genotype	Total # Cells	# Dying
0.75	+/+	158	0
	D/+	183	1
7	+/+	132	25
	D/+	153	22

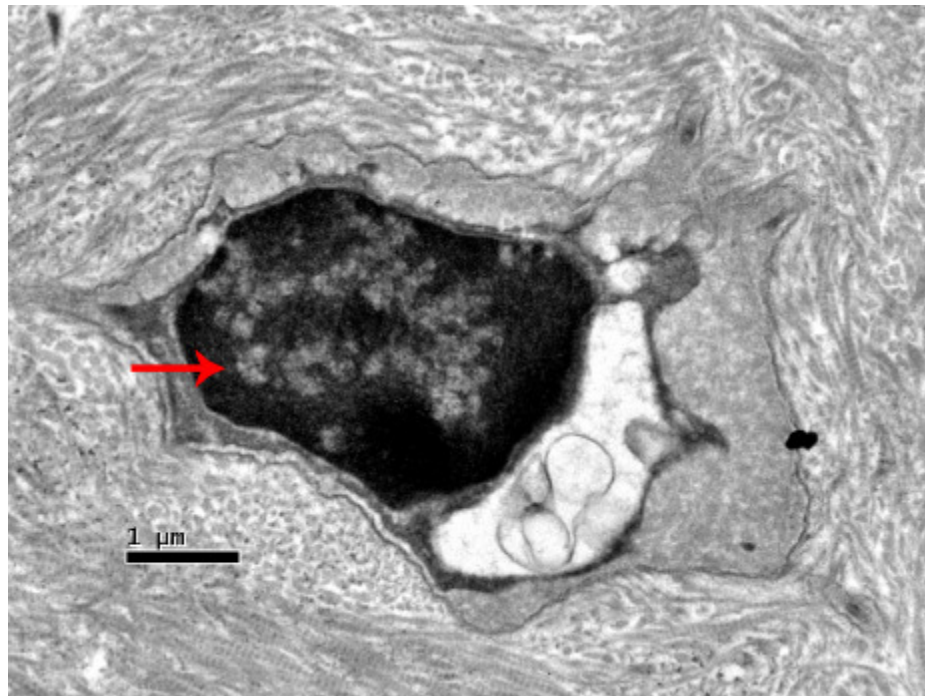


**Figure 25: Apoptotic cell** in a D/+ mouse at 9 months. Red arrow points to condensed chromatin. Collagen fibers are noticeably larger in calcified cartilage.

## DISCUSSION & FUTURE STUDIES

### **Area Fractions (ER, Matrix, Cell)**

Data from cell and matrix area fractions showed that mutants (D/+) invariably had higher cell fractions and lower matrix fractions compared to +/+ age matched controls if all ages are combined (Table 1, Figure 7). D/+ mice display a lower matrix fraction ( $p=.086$ ) even as early as 0 days, implying that proper matrix synthesis is hindered during fetal development. This is further evidenced in the perceivable difference in the matrix appearance in D/D mice at 0 months (Figure 15). D/D mice at 0 months had less visible collagen, but interestingly it did not have a significantly different matrix fraction from +/+ controls ( $p=.2047$ ). Studies on aging and OA in C57 black mice show no change in the cell fraction (chondrocyte density) with age, but a decrease in OA.<sup>42</sup> Unfortunately, no quantitative data on C57 black mice have been collected to support this claim. The current study shows decreases in cell fraction with both age and OA (D/+); the decrease is more rapid in D/+ mice and the cell fraction (chondrocyte density) is simply slightly higher than +/+ mice at each age (statistically significant at 0.75 months only) (Table 2). This implies that other proteins and water could be contributors to the statistically normal matrix fraction, but that the lack of collagen fibers leaves the matrix unable to withstand tensile and compressive forces placed on the joint. Biochemical studies on the matrix composition would be beneficial to determine how protein concentrations are changing in the articular cartilage of D/+ mice as OA advances.

ER area fractions at 0 days further support the idea that there is reduced collagen because the ER is significantly dilated in the D/D mice ( $p=.0081$ ) (Figure 15). It is quite likely that collagen is not secreted from the cells in D/D animals, so less collagen

surrounds the chondrocytes. Chondrocytes must be protected from the daily compressive and tensile forces they are exposed to, and in D/D mice this protection is severely compromised. The data from D/D animals validates the recent observations in fetal rib cartilage of the Dmm mouse: lower matrix fractions, higher cell fraction, dilated ER, and meager collagen fibrils in the matrix.<sup>31</sup>

The relationship between the +/+ and D/+ is a little more vague. Upon examination with the TEM, no morphological difference in the matrix structure and organization was documented at 0 days (Figure 15). Within age-groups, the only significant differences in matrix fractions seen between the +/+ and D/+ mice were at 0.75 months (Table 2). This outcome implies that because D/+ animals have one normal copy of the Col2A1 gene, at young ages they are still able to maintain a semi-normal matrix. Both genotypes (+/+ and D/+) at 0 and 0.75 months have a significantly higher ER fraction compared to older ages (1.5, 4, and 7 months) (Table 8, Figure 22), suggesting that some of the ER dilation at early stages in life is a normal developmental occurrence. This is further supported by data on normal human articular cartilage that shows an extensive ER is characteristic of cells actively synthesizing proteins.<sup>43</sup> Compared to the +/+ mice, D/+ animals do have a significantly dilated ER above the normal dilation at 0 and 0.75 months ( $p=.0113$  and  $p=.0063$  respectively) (Figure 15, Figure 18), and dilation of the ER is further pronounced in middle cells. Malfunctions in the protein secretory pathway, like those suspected in Dmm, have been linked to a phenomenon called ER stress.<sup>44</sup> The excessive dilations observed in D/+ mice at 0 and 0.75 months could contribute to ER stress, which is linked to decreased ECM production and chondrocyte apoptosis.<sup>44</sup> A higher ER fraction in D/+ mice compared to +/+ mice

persists until 7 months post-partum (not statistically significant), which could be a source of prolonged ER stress.

The significant dilation in the ER at 0 and 0.75 months in D/+ mice, therefore, suggests **1)** that abnormal collagen fibers are being retained inside of the cell to some degree leading to ER stress and **2)** that the excess dilation could be indicative of compensatory mechanisms that cause the good copy of the *Col2a1* gene to overproduce type II collagen. An excess of normal collagen fibers may be produced at early stages, and this production slows with age. Mutated fibers could be retained in the ER leading to distension of the ER and degraded intracellularly as the animal ages, or the mutated fibers could be secreted and degraded extracellularly. In either case, as the D/+ mice age the production of normal type II collagen slows, and persistent ER stress compounds the matrix deficiencies already present due to mutant collagen fibrils. As a result, insufficient normal matrix is produced in D/+ mice leading to premature OA. This is further evidenced in the fact that as the animals (+/+ and D/+) age, dilation of the ER in D/+ mice disappears (Figure 20, Figure 21, Figure 22). Furthermore, trends across age groups show that as the animals age, the difference in ER area fractions between the +/+ and D/+ merges to 0 by 7 months ( $p=1$ ) in the combined cell depths (Table 8, Figure 22). In middle cells at 7 months, although not statistically significant, the ER fraction of the D/+ is actually lower than the +/+. Because loss of dilations in the ER are suggested to be a sign of advanced OA,<sup>45</sup> it would be beneficial to see if the ER fraction in advanced OA of D/+ mice (12, 15, and 22 months) actually drops below the ER fraction of +/+ mice.

The lower matrix fraction shown in D/+ mice seems to support the idea that collagen is not properly secreted, causing expansion of the ER (larger cells) as collagen builds up inside, as previously observed in fetal rib cartilage of Dmm mice.<sup>31</sup> The data for this argument, however, would be indisputable if immuno-electron microscopy were carried out for Col2A1 in +/+ and D/+ mice at various ages. Helminen described ER dilations containing a proteinaceous material in a transgenic mouse line missing the type II pro-collagen gene, and other studies have demonstrated intracellular staining of Col2A1 in chondrocytes,<sup>8,9,11</sup> but no data are available that definitively show excess staining for Col2A1 in the ER of *Col2a1* mutants, including Dmm. Gold labeling would be one possible way of observing the distribution of Col2A1 intracellularly. Also, if a monoclonal antibody were developed specifically against the mutant collagen in Dmm, the distribution of normal and mutant fibrils could be documented.

### **Apoptosis**

Currently an on-going debate exists about the relevance of apoptosis in OA. Many suggest that apoptosis is a key hallmark of OA,<sup>33-35,37</sup> while others argue adamantly against it.<sup>46-48</sup> In the present study, apoptosis was more prevalent in older animals than in younger ones in both the +/+ and D/+ groups (Table 9). Furthermore, apoptotic cells were only observed in the calcified layer of articular cartilage. Both of these preliminary observations suggest that apoptosis is not a widespread phenomenon in OA in Dmm mice, consistent with findings on human osteoarthritic articular cartilage.<sup>48</sup> The data presented here are not sufficient to confirm or reject the presence of apoptosis as a sign of OA in Dmm. Additional data should be collected, especially since ER stress is suggested to lead to apoptosis,<sup>44</sup> in a light microscopy study using immunohistochemistry for

biomarkers of apoptosis. Two methods that could be used are terminal deoxynucleotidyl transferase-mediated dUTP nick end labeling (TUNEL) and insitu oligo ligation (ISOL). Neither technique is without flaws,<sup>46</sup> therefore using both methods would provide robust evidence to support or reject the presence of apoptosis in OA of Dmm mice.

### **Summary**

The data herein further validate Dmm as a model for OA. Furthermore, this study supports previous histological changes shown in the articular cartilage of Dmm<sup>30</sup> and recent changes observed in the fetal rib cartilage of Dmm.<sup>31</sup> Finding in the present study also suggest that the protein secretory pathway of Col2A1 in D/+ mice does not function properly which leads to a deficient matrix and premature OA. ER stress could be a major factor in the premature onset of OA in Dmm, but further studies on the composition of proteins in the ER and matrix are necessary to definitively conclude that type II collagen is retained in the ER. TEM characterizing the ER and cell structure should also be conducted at older ages in Dmm to show changes in advanced OA. Lastly, immunohistochemistry for apoptosis and other biomarkers of OA needs to be conducted on Dmm mice at various ages to further elucidate the pathological changes of OA.

## Bibliography

1. Teshima R, Otsuka T, Takasu N, Yamagata N, Yamamoto K. Structure of the most superficial layer of articular cartilage. *J Bone Joint Surg Br* 1995;77(3):460-4.
2. Buckwalter JA. Part I: Tissue Design and Chondrocyte-Matrix Interactions. *J Bone Joint Surg Am* 1997;79-A(4):600-611.
3. Reginato AM, Olsen BR. The role of structural genes in the pathogenesis of osteoarthritic disorders. *Arthritis Res* 2002;4(6):337-45.
4. Rodriguez RR, Seegmiller RE, Stark MR, Bridgewater LC. A type XI collagen mutation leads to increased degradation of type II collagen in articular cartilage. *Osteoarthritis Cartilage* 2004;12(4):314-20.
5. Steplewski A, Brittingham R, Jimenez SA, Fertala A. Single amino acid substitutions in the C-terminus of collagen II alter its affinity for collagen IX. *Biochem Biophys Res Commun* 2005;335(3):749-55.
6. Donahue LR, Chang B, Mohan S, Miyakoshi N, Wergedal JE, Baylink DJ, Hawes NL, Rosen CJ, Ward-Bailey P, Zheng QY and others. A missense mutation in the mouse *Col2a1* gene causes spondyloepiphyseal dysplasia congenita, hearing loss, and retinoschisis. *J Bone Miner Res* 2003;18(9):1612-21.
7. Kuivaniemi H, Tromp G, Prockop DJ. Mutations in fibrillar collagens (types I, II, III, and XI), fibril-associated collagen (type IX), and network-forming collagen (type X) cause a spectrum of diseases of bone, cartilage, and blood vessels. *Hum Mutat* 1997;9(4):300-15.
8. Chan D, Cole WG, Chow CW, Mundlos S, Bateman JF. A *COL2A1* mutation in achondrogenesis type II results in the replacement of type II collagen by type I and III collagens in cartilage. *J Biol Chem* 1995;270(4):1747-53.
9. Fernandes RJ, Seegmiller RE, Nelson WR, Eyre DR. Protein consequences of the *Col2a1* C-propeptide mutation in the chondrodysplastic *Dmm* mouse. *Matrix Biol* 2003;22(5):449-53.
10. Ito H, Rucker E, Steplewski A, McAdams E, Brittingham RJ, Alabyeva T, Fertala A. Guilty by association: some collagen II mutants alter the formation of ECM as a result of atypical interaction with fibronectin. *J Mol Biol* 2005;352(2):382-95.
11. Khetarpal U, Robertson NG, Yoo TJ, Morton CC. Expression and localization of *COL2A1* mRNA and type II collagen in human fetal cochlea. *Hear Res* 1994;79(1-2):59-73.
12. Pace JM, Li Y, Seegmiller RE, Teuscher C, Taylor BA, Olsen BR. Disproportionate micromelia (*Dmm*) in mice caused by a mutation in the C-propeptide coding region of *Col2a1*. *Dev Dyn* 1997;208(1):25-33.
13. Buckwalter JA, Martin J. Degenerative joint disease. *Clin Symp* 1995;47(2):1-32.
14. Pidd JG, Gardner DL, Adams ME. Ultrastructural changes in the femoral condylar cartilage of mature American foxhounds following transection of the anterior cruciate ligament. *J Rheumatol* 1988;15(4):663-9.
15. Gardner DL, Salter DM, Oates K. Advances in the microscopy of osteoarthritis. *Microsc Res Tech* 1997;37(4):245-70.
16. Sarzi-Puttini P, Cimmino MA, Scarpa R, Caporali R, Parazzini F, Zaninelli A, Atzeni F, Canesi B. Osteoarthritis: an overview of the disease and its treatment strategies. *Semin Arthritis Rheum* 2005;35(1 Suppl 1):1-10.

17. Buckwalter JA. Part II: Degeneration and Osteoarthritis, Repair, Regeneration, and Transplantation. *J Bone Joint Surg Am* 1997;79-A(4):612-632.
18. Huebner JL, Otterness IG, Freund EM, Caterson B, Kraus VB. Collagenase 1 and collagenase 3 expression in a guinea pig model of osteoarthritis. *Arthritis Rheum* 1998;41(5):877-90.
19. Martel-Pelletier J. Pathophysiology of osteoarthritis. *Osteoarthritis Cartilage* 1998;6(6):374-6.
20. Sandell LJ, Aigner T. Articular cartilage and changes in arthritis. An introduction: cell biology of osteoarthritis. *Arthritis Res* 2001;3(2):107-13.
21. van der Kraan PM, Stoop R, Meijers TH, Poole AR, van den Berg WB. Expression of type X collagen in young and old C57Bl/6 and Balb/c mice. Relation with articular cartilage degeneration. *Osteoarthritis Cartilage* 2001;9(2):92-100.
22. Buckwalter JA, Saltzman C, Brown T. The impact of osteoarthritis: implications for research. *Clin Orthop Relat Res* 2004(427 Suppl):S6-15.
23. Griffin TM, Guilak F. The role of mechanical loading in the onset and progression of osteoarthritis. *Exerc Sport Sci Rev* 2005;33(4):195-200.
24. Stickler GB, Belau PG, Farrell FJ, Jones JD, Pugh DG, Steinberg AG, Ward LE. Hereditary Progressive Arthro-Ophthalmopathy. *Mayo Clin Proc* 1965;40:433-55.
25. Spranger J, Winterpacht A, Zabel B. The type II collagenopathies: a spectrum of chondrodysplasias. *Eur J Pediatr* 1994;153(2):56-65.
26. Foster MJ, Caldwell AP, Staheli J, Smith DH, Gardner JS, Seegmiller RE. Pulmonary hypoplasia associated with reduced thoracic space in mice with disproportionate micromelia (DMM). *Anat Rec* 1994;238(4):454-62.
27. Seegmiller RE, Brown K, Chandrasekhar S. Histochemical, immunofluorescence, and ultrastructural differences in fetal cartilage among three genetically distinct chondrodystrophic mice. *Teratology* 1988;38(6):579-92.
28. Fernandes RJ, Seegmiller RE, Nelson WR, Eyre DR. Protein consequences of the Col2a1 C-propeptide mutation in the chondrodysplastic Dmm mouse. *Matrix Biol* 2003;22(5):449-453.
29. Brown KS, Cranley RE, Greene R, Kleinman HK, Pennypacker JP. Disproportionate micromelia (Dmm): an incomplete dominant mouse dwarfism with abnormal cartilage matrix. *Journal of Embryology and Experimental Morphology* 1981;62:165-182.
30. Bomsta BD, Bridgewater LC, Seegmiller RE. Premature osteoarthritis in the Disproportionate micromelia (Dmm) mouse. *Osteoarthritis Cartilage* 2006;14(5):477-85.
31. Seegmiller RE, Bomsta BD, Bridgewater LC, Niederhauser CM, Montano C, Sudweeks S, Eyre DR, Fernandes RJ. The Heterozygous Disproportionate micromelia (Dmm) Mouse: Morphological Changes in Fetal Cartilage Precede Postnatal Dwarfism and Compared to Lethal Homozygotes Can Explain the Mild Phenotype. *J Histochem Cytochem* 2008.
32. Helminen HJ, Kiraly K, Pelttari A, Tammi MI, Vandenberg P, Pereira R, Dhulipala R, Khillan JS, Ala-Kokko L, Hume EL and others. An inbred line of transgenic mice expressing an internally deleted gene for type II procollagen



- (COL2A1). Young mice have a variable phenotype of a chondrodysplasia and older mice have osteoarthritic changes in joints. *J Clin Invest* 1993;92(2):582-95.
33. Heraud F, Heraud A, Harmand MF. Apoptosis in normal and osteoarthritic human articular cartilage. *Ann Rheum Dis* 2000;59(12):959-65.
  34. Kouri JB, Aguilera JM, Reyes J, Lozoya KA, Gonzalez S. Apoptotic chondrocytes from osteoarthrotic human articular cartilage and abnormal calcification of subchondral bone. *J Rheumatol* 2000;27(4):1005-19.
  35. Mistry D, Oue Y, Chambers MG, Kayser MV, Mason RM. Chondrocyte death during murine osteoarthritis. *Osteoarthritis Cartilage* 2004;12(2):131-41.
  36. Okazaki R, Sakai A, Ootsuyama A, Sakata T, Nakamura T, Norimura T. Apoptosis and p53 expression in chondrocytes relate to degeneration in articular cartilage of immobilized knee joints. *J Rheumatol* 2003;30(3):559-66.
  37. Hashimoto S, Ochs RL, Komiya S, Lotz M. Linkage of chondrocyte apoptosis and cartilage degradation in human osteoarthritis. *Arthritis Rheum* 1998;41(9):1632-8.
  38. Chen CT, Burton-Wurster N, Borden C, Hueffer K, Bloom SE, Lust G. Chondrocyte necrosis and apoptosis in impact damaged articular cartilage. *J Orthop Res* 2001;19(4):703-11.
  39. Ricks JE, Ryder VM, Bridgewater LC, Schaalje B, Seegmiller RE. Altered mandibular development precedes the time of palate closure in mice homozygous for disproportionate micromelia: an oral clefting model supporting the Pierre-Robin sequence. *Teratology* 2002;65(3):116-20.
  40. Spurr AR. A low-viscosity epoxy resin embedding medium for electron microscopy. *J Ultrastruct Res* 1969;26(1):31-43.
  41. Reynolds ES. The use of lead citrate at high pH as an electron-opaque stain in electron microscopy. *J Cell Biol* 1963;17:208-12.
  42. Yamamoto K, Shishido T, Masaoka T, Imakiire A. Morphological studies on the ageing and osteoarthritis of the articular cartilage in C57 black mice. *J Orthop Surg (Hong Kong)* 2005;13(1):8-18.
  43. Weiss C, Rosenberg L, Helfet AJ. An ultrastructural study of normal young adult human articular cartilage. *J Bone Joint Surg Am* 1968;50(4):663-74.
  44. Yang L, Carlson SG, McBurney D, Horton WE, Jr. Multiple signals induce endoplasmic reticulum stress in both primary and immortalized chondrocytes resulting in loss of differentiation, impaired cell growth, and apoptosis. *J Biol Chem* 2005;280(35):31156-65.
  45. Weiss C. Ultrastructural characteristics of osteoarthritis. *Fed Proc* 1973;32(4):1459-66.
  46. Aigner T. Apoptosis, necrosis, or whatever: how to find out what really happens? *J Pathol* 2002;198(1):1-4.
  47. Aigner T. Chondrocyte apoptosis in osteoarthritis: comment on the letter by Kouri and Abbud-Lozoya. *Arthritis Rheum* 2003;48(4):1166-7.
  48. Aigner T, Hemmel M, Neureiter D, Gebhard PM, Zeiler G, Kirchner T, McKenna L. Apoptotic cell death is not a widespread phenomenon in normal aging and osteoarthritis human articular knee cartilage: a study of proliferation, programmed cell death (apoptosis), and viability of chondrocytes in normal and osteoarthritic human knee cartilage. *Arthritis Rheum* 2001;44(6):1304-12.

## Curriculum Vitae

### Crystal Noelle Smaldone

Brigham Young University  
Department of Physiology and Developmental Biology  
574 Widtsoe Building  
Provo, UT 84602  
[buggy@byu.net](mailto:buggy@byu.net)

#### Education:

M.S., Physiology and Developmental Biology, Brigham Young University, 2008  
Concentrations: Transmission Electron Microscopy, Articular Cartilage  
Thesis: Cellular and Matrix Changes in Articular Cartilage of the Disproportionate Micromelia Mouse Model of Osteoarthritis

B.S., Biology, Brigham Young University, Provo, UT, 2005

#### Experience:

Lab Instructor, September 2005 – June 2008  
Brigham Young University  
Course: Essentials of Human Physiology Lab

Teaching Assistant, January – April 2006, September – December 2007  
Brigham Young University  
Course: Developmental Biology

Research Assistant, April 2004 – June 2005  
Brigham Young University, Supervisor: Dr. Dennis K. Shiozawa  
Emphasis: DNA sequencing, Aquatic vertebrates and invertebrates, Phylogenetics

Research Assistant,  
Brigham Young University, Supervisor: Dr. David A. McClellan  
Emphasis: Phylogenetics

#### Research Skills:

Extensive experience in transmission electron microscopy, genotyping, DNA sequencing. Other experience includes immunohistochemistry, tomography, and Dual beam FIB.

#### Presentations:

Phylogenetic Relationships of *Cottus beldingi* in the Basin and Range and Colorado Plateau of Western North America. Oral presentation at the North American Benthological Society Meetings 2005 (New Orleans, LA).

#### Skills and Qualifications:

Microsoft Office  
Adobe Photoshop  
Image J (NIH)

#### References:

Excellent references available upon request.